

See discussions, stats, and author profiles for this publication at: <https://www.researchgate.net/publication/260991235>

"Click" Synthesis of Intrinsically Hydrophilic Dendrons and Dendrimers Containing Metal Binding Moieties at Each Branching Unit

ARTICLE in MACROMOLECULES · MARCH 2014

Impact Factor: 5.8 · DOI: 10.1021/ma500126f

CITATIONS

5

READS

45

5 AUTHORS, INCLUDING:



[David J Kiemle](#)

State University of New York College of Enviro...

31 PUBLICATIONS 301 CITATIONS

[SEE PROFILE](#)



[Connor Boyle](#)

University of Massachusetts Amherst

3 PUBLICATIONS 6 CITATIONS

[SEE PROFILE](#)



[Eoghan Leif Connors](#)

Stony Brook University

2 PUBLICATIONS 5 CITATIONS

[SEE PROFILE](#)



[Ivan Gitsov](#)

State University of New York College of Enviro...

90 PUBLICATIONS 3,142 CITATIONS

[SEE PROFILE](#)

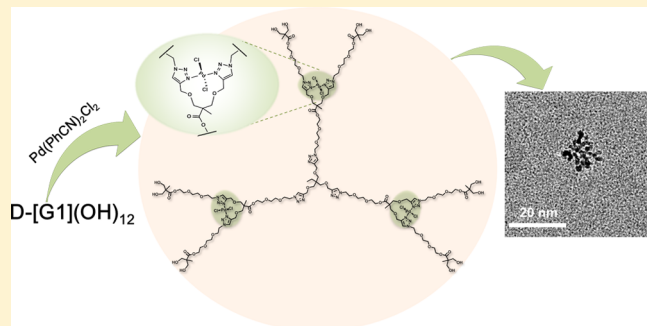
"Click" Synthesis of Intrinsically Hydrophilic Dendrons and Dendrimers Containing Metal Binding Moieties at Each Branching Unit

Lili Wang,[†] David J. Kiemle,[†] Connor J. Boyle,[†] Eoghan L. Connors,[†] and Ivan Gitsov*,^{†,‡}

[†]Department of Chemistry and [‡]The Michael M. Szwarc Polymer Research Institute, State University of New York-ESF, Syracuse, New York 13210, United States

Supporting Information

ABSTRACT: A new family of water-soluble triazole dendrimers composed of tri(ethylene glycol) (TrEG) and bis(methyloxypropionic acid (bis-MPA) was created through Cu(I)-catalyzed alkyne–azide cycloaddition (CuAAC) between specifically designed complementary building blocks. Dendrimers up to generation three were synthesized by CuAAC to a trifunctional core with yields ranging from 72% for generation one, through 67% for generation two, and 64% for third generation dendrimer. The two triazole rings at each bis-MPA branching site could serve as efficient chelating pockets for some VIIIA group elements. As proof-of-principle, the $[\text{PdCl}_2(\text{PhCN})_2]$ coordination chemistry of these hydrophilic dendritic ligands was studied by ¹H NMR, dynamic light scattering, transmission electron microscopy, and DFT calculations. The results showed that the complexation is completed within 5 min. The novel hydrophilic dendritic Pd complexes were able to catalyze Suzuki–Miyaura coupling reactions in water within 3 h at 100 °C, at 60 °C, and even at 50 °C with practically quantitative conversion.



INTRODUCTION

Dendrimers are perfectly branched and monodisperse macromolecules with layered architecture. By regulating dendrimer synthesis, it is possible to precisely manipulate both their molecular weight and chemical composition, thereby inducing predictable properties and diverse applications.¹ The two major synthetic approaches for constructing dendrimers are the divergent² and convergent methods.³ It should be mentioned that both strategies require efficient and high yield reactions in order to produce macromolecular structures with defect-free architecture. Therefore, the development of effective synthetic strategies toward dendrimers with sophisticated architecture and broad application potential is a continuing theme in dendrimer synthesis. Among those efficient approaches to dendrimers, the Huisgen cycloaddition⁴ is increasingly used. The copper-catalyzed azide–alkyne cycloaddition (CuAAC), introduced in 2001, could be considered as a variation of this method.⁵ Since then, it attracted considerable attention for the reason that it is quantitative and robust process, which is functional-group tolerant, and can proceed under mild conditions. These features make the "click" reaction particularly suitable for the synthesis of dendrimers as shown initially by Wu et al. and others.⁶ Currently CuAAC is used in a broad array of dendrimer syntheses and modifications.⁷

Notably, the major interest in the CuAAC is due to the fact that it is an efficient synthetic approach to covalently link functional building blocks through the formation of a 1,4-disubstituted 1,2,3-triazole ring, which is rather stable under various conditions.

Despite some early attempts and prognoses,⁸ until recently little attention was focused on exploiting the benefits of the triazole moiety outside its simple linking functions.⁹ Most application attempts associated with this group occurred outside the dendrimer/polymer "domain" and were centered on the investigation of the coordination properties of small triazole heterocycles to transitional metal ions. It was shown that the 1,2,3-triazole ring could serve as a ligand, which can provide suitable coordination sites via nitrogens N3⁸ and/or N2^{9,10} or through C4 as carbene¹¹ to transitional metals such as Pd,^{10a,c} Cu,¹² Pt,¹³ Re,^{11c,9b,14} and Ag.^{11a,14} Among those complexes, the palladium complex is of specific interest because of its catalytic properties in various cross-coupling organic reactions. Pd-mediated catalysis has provided a general and mild procedure for carbon–carbon bond construction.¹⁵ Palladium-containing dendrimers have long been used as promising catalysts for these reactions,¹⁸ but studies on triazole-containing polymers as Pd ligands and catalysts in C–C couplings are relatively rare.^{19,20} Interesting current investigations also suggest that the modification of dendrimer periphery with short poly(ethylene glycol) chains might favorably affect the activity and stability of dendritic palladium catalysts in Suzuki–Miyaura reactions.²¹

The motivation for this study originates from these publications.^{19,21} Herein, we report the convergent synthesis

Received: January 16, 2014

Revised: March 5, 2014

Published: March 17, 2014

and characterization of a new family of water-soluble triazole dendrimers composed of triethylene glycol, TrEG, as the water-soluble interior spacer and bis(methyloxy)propionic acid, bis-MPA, as the branching unit. Dendrons and dendrimers up to generation 3 are produced by iterative coupling/modification involving alkyne–azide “click” reactions with novel AB₂ monomers. The resulting TrEG/bis-MPA-based triazole dendrimers are freely water-soluble and show promising metal ion binding abilities. Model Suzuki–Miyaura cross-coupling reactions confirm the high catalytic activity of their Pd complexes in aqueous media.

EXPERIMENTAL SECTION

Materials. 2-[2-(2-Chloroethoxy)ethoxy]ethanol (96%); *p*-toluenesulfonic acid monohydrate ($\geq 98.5\%$); sodium hydride, NaH (95%, dry powder); N,N,N',N"-pentamethyldiethylenetriamine, PMDETA (99%); copper(I) bromide, CuBr (98%); 1,1,1-tris(hydroxymethyl)-propane (97%); propargyl bromide (80 wt % in toluene); N,N'-dicyclohexylcarbodiimide, DCC (99%); and trifluoroacetic acid, TFA (99%), were all purchased from Sigma-Aldrich and used as received. 2,2-Bis(hydroxymethyl)propionic acid, bis-MPA (99+%), and sodium azide, NaN₃ (98%, powder), were purchased from Acros and used as received. Dichlorobis(benzonitrile)palladium, Pd(PhCN)₂Cl₂ (99%), and ethyl acetate, EtOAc (reagent grade), were purchased from Strem Chemicals, Inc., and Pharmco, respectively, and used without further purification. 4-(Dimethylamino)pyridinium *p*-toluenesulfonate (DPTS) was synthesized using the procedure developed by Moore and Stupp.²²

Instrumentation. Size exclusion chromatography (SEC) analyses were performed on a line consisting of a Waters M510 pump, a Waters U6K universal injector, three 5 μ m PL Gel columns (50 \AA , 500 \AA , and Mixed C), and a Viscotek 250 dual refractive index/viscometry detector. The separation was achieved at 40 °C with freshly distilled tetrahydrofuran (THF) eluting at 1 mL/min. The apparent molecular masses and molecular mass distributions were determined using 20 monodisperse poly(styrene) standards (162 Da–200 kDa) and Viscotek OmniSEC 3.1 software.

The mass spectrometric measurements were made on a Bruker Autoflex III MALDI-TOF MS instrument with Smartbeam ion source equipped with a Nd:YAG laser (266 and 355 nm). All spectra were acquired using a reflect-positive mode. The laser attenuation was set to the lowest value possible to get high resolution spectra. Matrix was prepared by dissolving recrystallized 2,5-dihydroxybenzoic acid (DHB) in methanol at a concentration of 40 mg/mL. Sample was prepared in methanol at a concentration of 1 mg/mL. Samples were spotted using the dried-droplet method, where sample and matrix were premixed with a ratio of 1:7. 1 μ L of mixed solution was spotted on an AnchorChip target plate (MTP 384 polished steel, Bruker Daltonics).

¹H NMR and ¹³C NMR spectra were recorded using CDCl₃ or DMSO-*d*₆ as solvents with Bruker AVANCE 300 or 600 MHz instruments. ¹H–¹H 2D gradient enhanced homonuclear correlation spectroscopy (ge-COSY) NMR experiments were performed using a delay time of 1.9 s, obtaining 128 increments and 1 scans per increment, within a spectral width of 4807 Hz operating at 600 MHz. The DEPT edited heteronuclear single quantum coherence spectroscopy (DEPT-HSQC) experiments were executed using a delay time of 2 s, obtaining 256 increments and 4 scans per increment, within spectral widths of 7212 Hz (¹H) and 25 000 Hz (¹³C) and operating at 125 and 600 MHz.

The DLS measurements were performed on a Malvern Zetasizer ZS instrument. The instrument was equipped with a 633 nm laser source and a backscattering detector at 173°. Data were analyzed using a CONTIN procedure.

TEM measurements were performed on JEOL 2000EX instrument operated at 100 kV with a tungsten filament. A drop of sample solution at a concentration of 0.5–1 mg/mL was placed on a carbon-coated 400 square mesh copper grid. Excess of solution was blotted with a lint-free filter paper after 1 min, and the grid was allowed to dry under ambient temperature.

The palladium concentration in solution was determined on a PerkinElmer Elan DRC-e inductively coupled plasma mass spectrometer (ICP-MS).

Syntheses. **2,2-Bis(propargyl)propargyl Propionate (1).** Bis-MPA (1.63 g, 12.16 mmol) was dissolved with 15 mL of dry DMF in a flame-dried two-neck flask. The system was cooled to 0 °C, and NaH (964 mg, 40.2 mmol) was added carefully at once. The reaction mixture was stirred until hydrogen evolution was complete. Then, propargyl bromide (80 wt % in toluene, 8.75 g, 58.8 mmol) was added slowly. The mixture was stirred at 0 °C for 30 min and then at room temperature (RT) for 12 h. The reaction was quenched with 10 mL of water and extracted with EtOAc (3 \times 50 mL). The organic layers were combined, washed with brine, dried over MgSO₄, and concentrated to give a dark brown oily product (1.01 g, 34%). ¹H NMR (300 MHz, CDCl₃) δ , ppm: 1.25 (s, 3H), 2.42 (t, J = 2.4 Hz, 2H), 2.46 (t, J = 2.5 Hz, 1H), 3.67 (s, 2H), 4.15 (d, J = 2.4 Hz, 4H), 4.70 (d, J = 2.5 Hz, 2H).

2,2-Bis(propargyl)propionic Acid (2). **1** (877.45 mg, 3.53 mmol) was dissolved in 30 mL of THF and 5 mL of H₂O at 0 °C in a two-neck flask. Then 25 mL of LiOH-H₂O (0.67 N) was slowly added to the flask. The completion of the reaction was monitored by TLC. After completion, the reaction mixture was cooled to 0 °C, neutralized with 2 M HCl, and extracted with EtOAc (3 \times 30 mL). The organic layers were combined and washed with brine. EtOAc was evaporated off, and the crude product was purified by column chromatography with hexane/EtOAc (53/47 v/v) to give pale yellow oil (571.26 mg, 77%). T_g = -42.2 °C. ¹H NMR (300 MHz, CDCl₃) δ : 4.17 (d, J = 2.4 Hz, 4H), 3.67 (d, J = 0.8 Hz, 4H), 2.43 (t, J = 2.3 Hz, 2H), 1.25 (s, 3H). ¹³C NMR (75 MHz, CDCl₃) δ : 179.87, 79.34, 74.58, 71.46, 58.70, 47.77, 17.79.

2,2-Bis(propargyl)-2-[2-(2-chloroethoxy)ethoxy]ethyl Propionate (3). **2** (970.55 mg, 4.62 mmol), 2-[2-(2-chloroethoxy)ethoxy]ethanol (932.05 mg, 5.54 mmol), and DPTS (272.24 mg, 0.93 mmol) were dissolved in 15 mL of dry CH₂Cl₂. After the reaction system was degassed with argon, 1.34 g of DCC (6.49 mmol) was added. The reaction mixture was stirred at RT overnight under argon. After the reaction was completed, the dicyclohexyl urea (DCU) formed, was filtered, and washed with CH₂Cl₂. The crude product was purified by flash chromatography on silica gel with eluting solvent of EtOAc/hexane (33/67, v/v) to give **3** as colorless oily product (1.38 g, 84%). T_g = -61.9 °C. ¹H NMR (600 MHz, CDCl₃) δ : 4.30 (t, J = 4.8 Hz, 2H), 4.17 (d, J = 2.3 Hz, 4H), 3.79 (t, J = 5.9 Hz, 2H), 3.73 (t, J = 4.8 Hz, 2H), 3.71–3.62 (m, 10H), 2.44 (t, J = 2.3 Hz, 2H), 1.26 (s, 3H). ¹³C NMR (151 MHz, CDCl₃) δ : 174.08, 79.71, 74.33, 71.77, 71.44, 70.73, 70.63, 69.19, 63.81, 58.67, 48.05, 42.72, 17.85.

Isopropylidene-2,2-bis(methoxy)propionic Acid (IBPA) (4). Bis-MPA (21.15 g, 157.8 mmol), 2,2-dimethoxypropane (29 mL, 235.0 mmol), and *p*-toluenesulfonic acid monohydrate were dissolved in 100 mL of dry acetone. The reaction mixture was stirred overnight at RT under argon. Then 1 mL of NH₃/EtOH (1/1, v/v) solution was added to quench the catalyst. The solvent was evaporated, and the crude product was then dissolved in 250 mL of CH₂Cl₂ and extracted three times with deionized H₂O (50 mL). The organic layer was dried over MgSO₄ and concentrated to give the target compound as white solid (24.21 g, 88%). ¹H NMR (600 MHz, DMSO) δ : 4.03 (d, J = 11.6 Hz, 2H), 3.56 (d, J = 11.6 Hz, 2H), 1.35 (s, 3H), 1.28 (s, 3H), 1.10 (s, 3H). ¹³C NMR (151 MHz, DMSO) δ : 175.92, 97.74, 64.43, 41.22, 24.93, 23.40, 18.90.

Isopropylidene-2,2-bis(methoxy)-2-[2-(2-chloroethoxy)]ethyl Propionate (5). **4** (3.060 g, 17.6 mmol), 2-[2-(2-chloroethoxy)ethoxy]ethanol (2.864 g, 17.0 mmol), and DPTS (0.997 g, 3.39 mmol) were dissolved in 20 mL of CH₂Cl₂. After the reaction flask was degassed with argon, DCC (4.037 g, 19.6 mmol) was added. The reaction mixture was stirred at RT overnight under an argon atmosphere. After the reaction was completed, DCU was filtered and washed with CH₂Cl₂. The crude product was purified by column chromatography eluting with EtOAc/hexane (33/67, v/v). The solvent was removed to obtain **5** as colorless oil (4.59 g, 81%). T_g = -66.3 °C. ¹H NMR (600 MHz, CDCl₃) δ : 4.32 (m, J = 4.8 Hz, 2H), 4.22 (d, J = 11.7 Hz, 2H), 3.77 (t, J = 5.9 Hz, 2H), 3.74 (t, J = 4.8 Hz, 2H), 3.71–3.61 (m, 8H), 1.45 (s, 3H), 1.40 (s, 3H), 1.25 (s, 3H). ¹³C NMR (151 MHz, CDCl₃) δ : 174.16, 98.07, 71.42, 70.71, 70.62, 69.11, 65.97, 63.86, 42.68, 41.84, 24.24, 23.07, 18.70.

Isopropylidene-2,2-bis(methoxy)-2-[2-(2-azideethoxy)]ethyl Propionate (6). **5** (3.116 g, 9.60 mmol) and **NaN₃** (3.203 g, 49.3 mmol) were dissolved in 15 mL of DMF. The reaction was allowed to react at 60 °C for 18 h under argon. The slurry was cooled to RT followed by adding 10 mL of water. The mixture was extracted with EtOAc (3 × 50 mL), and the combined organic layers were washed twice with 50 mL of brine and dried over MgSO₄. EtOAc was removed under vacuum to yield **6** (2.874 g, 91%) as colorless oil. $T_g = -73.2$ °C. ¹H NMR (600 MHz, CDCl₃) δ: 4.33 (t, $J = 4.8$ Hz, 2H), 4.22 (d, $J = 11.8$ Hz, 2H), 3.75 (t, $J = 4.8$ Hz, 2H), 3.72–3.64 (m, 8H), 3.41 (t, $J = 5.0$ Hz, 2H), 1.45 (s, 3H), 1.41 (s, 3H), 1.25 (s, 3H). ¹³C NMR (151 MHz, CDCl₃) δ: 174.16, 98.07, 70.75, 70.68, 70.10, 69.14, 65.97, 63.88, 50.71, 41.83, 24.18, 23.14, 18.70.

Synthesis of Cl-[G1] (7). In a typical “click” reaction, a flask sealed with a rubber septum was charged with **3** (1.280 g, 3.55 mmol) and **6** (2.414 g, 7.28 mmol) in 4 mL of DMF. The reaction system was degassed by three freeze–pump–thaw cycles and backfilled with argon. Then, CuBr (1.184 g, 8.16 mmol) was added under argon followed by addition of PMDETA (1.372 g, 7.93 mmol) via an argon-purged syringe. The mixture was further degassed by two freeze–pump–thaw cycles and stirred under argon at RT for 24 h. After completion, the mixture was passed through a short column of aluminum oxide twice, using EtOAc as eluent to remove the copper catalyst. The product was further purified by flash chromatography eluting with methanol/EtOAc (5/95, v/v). Colorless oil (3.266 g, 87%) was obtained after removing the solvent. $T_g = -32.3$ °C. ¹H NMR (600 MHz, CDCl₃) δ: 7.70 (s, 2H), 4.63 (s, 4H), 4.55 (t, $J = 5.2$ Hz, 4H), 4.32 (t, $J = 5.0$, 4H), 4.25 (t, $J = 5.0$, 2H), 4.21 (d, $J = 11.8$ Hz, 4H), 3.90 (t, $J = 5.2$ Hz, 4H), 3.76 (t, $J = 5.8$ Hz, 2H), 3.73–3.58 (m, 20H), 1.43 (s, 6H), 1.38 (s, 6H), 1.22 (s, 6H), 1.21 (s, 3H). ¹³C NMR (151 MHz, CDCl₃) δ: 174.24, 174.12, 145.02, 123.52, 98.05, 72.14, 71.36, 70.65, 70.58, 70.54, 70.47, 69.51, 69.10, 69.04, 65.95, 65.00, 63.77, 63.69, 50.15, 48.31, 42.76, 41.84, 24.58, 22.73, 18.66, 17.90. MS (MALDI-TOF MS, positive mode): calculated for C₄₅H₇₅ClN₆O₁₈: [M]⁺ *m/z* = 1023.48. Found: [M + Na]⁺ *m/z* = 1045.55.

Synthesis of N₃-[G1]. **7** (2.307 g, 2.24 mmol) and **NaN₃** (916 mg, 14.1 mmol) were dissolved in 6 mL of DMF. The reaction was left at 60 °C for 24 h under argon. Then, the system was cooled down to RT followed by adding 10 mL of water and extracted with ethyl acetate (3 × 30 mL). All organic layers were combined, washed with 30 mL of brine twice, and dried over MgSO₄. The solvent was evaporated to give product as colorless oil (2.272 g, 98%). ¹H NMR (600 MHz, CDCl₃) δ: 7.66 (s, 2H), 4.60 (s, 4H), 4.51 (t, $J = 5.3$ Hz, 4H), 4.28 (t, $J = 4.9$ Hz, 4H), 4.22 (t, $J = 5.0$ Hz, 4H), 4.17 (d, $J = 11.8$ Hz, 4H), 3.87 (t, $J = 5.3$ Hz, 4H), 3.69–3.56 (m, 28H), 3.37 (t, $J = 5.2$ Hz, 4H), 1.42 (s, 6H), 1.37 (s, 6H), 1.18 (s, 6H), 1.17 (s, 3H). ¹³C NMR (151 MHz, CDCl₃) δ: 174.23, 174.11, 145.04, 123.50, 98.06, 72.13, 70.69, 70.61, 70.58, 70.48, 70.05, 69.52, 69.13, 69.05, 65.96, 65.02, 63.78, 63.70, 60.36, 50.68, 50.16, 48.31, 41.85, 24.56, 21.02, 18.67, 17.90. MS (MALDI-TOF MS, positive mode): calculated for C₄₅H₇₅N₉O₁₈: [M]⁺ *m/z* = 1029.52. Found: [M + Na]⁺ *m/z* = 1052.61.

Synthesis of Cl-[G2]. A flask, sealed with a rubber septum, was charged with N₃-[G1] (1.78 g, 1.73 mmol) and **3** (302.41 mg, 0.84 mmol) dissolving in 2 mL of DMF. The reaction system was degassed by three freeze–pump–thaw cycles and backfilled with argon. Then, CuBr (648 mg, 4.47 mmol) was added under argon followed by PMDETA addition (766 mg, 4.52 mmol) with an argon-purged syringe through the septum. The reaction system was further degassed by two freeze–pump–thaw cycles. The reaction was left to stir under argon at RT. After completion, the mixture was passed through a short column of aluminum oxide twice eluting with methanol and EtOAc. The product was further purified by flash chromatography on silica gel eluting with 20/80 methanol/EtOAc. Colorless oil (1.64 g, 81%) was obtained after evaporating off the solvent. $T_g = -26.8$ °C. ¹H NMR (600 MHz, CDCl₃) δ: 7.70 (m, 6H), 4.62 (s, 12H), 4.54 (t, $J = 5.2$ Hz, 12H), 4.35–4.28 (m, 8H), 4.27–4.22 (m, 6H), 4.21 (d, $J = 11.8$ Hz, 8H), 3.89 (m, 12H), 3.76 (t, $J = 5.8$ Hz, 2H), 3.73–3.56 (m, 64H), 1.44 (s, 12H), 1.39 (s, 12H), 1.23–1.17 (m, 21H). ¹³C NMR (151 MHz, CDCl₃) δ: 174.42, 174.13, 144.98, 123.56, 98.07, 72.20, 72.14, 71.36, 70.66, 70.58, 70.55, 70.49, 70.46, 69.51, 69.11, 69.06, 65.97, 65.00, 63.79, 63.71, 63.62, 50.16, 48.31,

42.80, 41.87, 24.59, 22.75, 18.68, 17.92. MS (MALDI-TOF MS, positive mode): calculated for C₁₀₇H₁₇₅ClN₁₈O₄₂: [M]⁺ *m/z* = 2420.18. Found: [M + Na]⁺ *m/z* = 2442.11.

Synthesis of N₃-[G2]. Cl-[G2] (1.50 g, 0.62 mmol) and **NaN₃** (204.23 mg, 3.14 mmol) were dissolved in 5 mL of DMF. The reaction was allowed to react at 60 °C under argon. The completion of the reaction was monitored via MALDI-TOF MS. Then, the reaction mixture was cooled to RT followed by addition of 10 mL of water and extraction with EtOAc (3 × 30 mL). All organic layers were combined, washed twice with 30 mL of brine, and dried over MgSO₄. The solvent was removed to give the product as colorless oil (1.385 g, 92%). ¹H NMR (600 MHz, CDCl₃) δ: 7.70 (s, 6H), 4.62 (s, 12H), 4.54 (t, $J = 5.2$ Hz, 12H), 4.34–4.29 (m, 8H), 4.24 (m, 6H), 4.21 (d, $J = 11.8$ Hz, 8H), 3.89 (m, 12H), 3.75–3.55 (m, 64H), 3.40 (t, $J = 5.0$ Hz, 2H), 1.45 (s, 12H), 1.39 (s, 12H), 1.25–1.14 (m, 21H). ¹³C NMR (151 MHz, CDCl₃) δ: 174.22, 174.14, 144.98, 123.56, 98.07, 72.19, 72.13, 70.58, 70.55, 70.49, 70.46, 69.52, 69.50, 69.06, 65.97, 65.00, 63.79, 63.62, 50.69, 50.16, 48.31, 41.87, 24.59, 22.66, 18.68, 17.91. MS (MALDI-TOF MS, positive mode): calculated for C₁₀₇H₁₇₅N₂₁O₄₂: [M]⁺ *m/z* = 2426.22. Found: [M + Na]⁺ *m/z* = 2449.81.

Synthesis of Cl-[G3]. A flask sealed with a rubber septum was charged with N₃-[G2] (756 mg, 0.31 mmol) in 1.5 mL of DMF and 54 mg of **3** in 533 μL of DMF from a stock solution (0.15 mmol). The reaction system was degassed by three freeze–pump–thaw cycles and backfilled with argon. Then, CuBr (91 mg, 0.63 mmol) was added under argon followed by PMDETA addition (106 mg, 0.62 mmol) with an argon purged syringe through the septum. Two freeze–pump–thaw cycles was performed to degas the system, which was left stirring at RT under argon. After completion, the mixture was passed twice through a short column of aluminum oxide using methanol and EtOAc as eluent. The crude product was purified using flash chromatography eluting with methanol/EtOAc (33/67, v/v) to give colorless oil (560 mg, 72%). $T_g = -24.8$ °C. ¹H NMR (600 MHz, CDCl₃) δ: 7.70 (s, 14H), 4.62 (m, 28H), 4.54 (t, $J = 4.7$ Hz, 28H), 4.37–4.27 (m, 16H), 4.26–4.22 (m, 14H), 4.21 (d, $J = 11.8$ Hz, 16H), 3.89 (m, 28H), 3.76 (t, $J = 5.9$ Hz, 2H), 3.72–3.55 (m, 136H), 1.45 (s, 24H), 1.39 (s, 24H), 1.24–1.15 (m, 45H). ¹³C NMR (151 MHz, CDCl₃) δ: 174.09, 144.92, 123.55, 98.07, 72.12, 70.58, 70.54, 70.49, 70.45, 69.51, 69.06, 65.97, 64.99, 63.79, 63.62, 50.16, 50.12, 41.87, 24.61, 22.74, 18.68, 17.93. MS (MALDI-TOF MS, positive mode): calculated for C₂₃H₃₇N₄₂O₉₀: [M]⁺ *m/z* = 5215.58. Found: [M + Na]⁺ *m/z* = 5241.26.

Synthesis of N₃-[G3]. Cl-[G3] (450 mg, 86 μmol) and **NaN₃** (180 mg, 2.77 mmol) were dissolved in 3 mL of DMF. The reaction was allowed to proceed at 60 °C under argon. After completion, the reaction mixture was cooled to RT, followed by the addition of 10 mL of water. The mixture was extracted with EtOAc (3 × 20 mL). All organic layers were combined and washed with 20 mL of brine. The solvent was removed to give the desired product as colorless oil (396 mg, 88%). ¹H NMR (600 MHz, CDCl₃) δ: 7.70 (s, 14H), 4.62 (m, 28H), 4.54 (t, $J = 5.1$ Hz, 28H), 4.34–4.29 (m, 16H), 4.24 (m, 14H), 4.21 (d, $J = 11.8$ Hz, 16H), 3.89 (m, 28H), 3.72–3.56 (m, 136H), 3.39 (t, $J = 5.0$ Hz, 2H), 1.44 (s, 24H), 1.39 (s, 24H), 1.24–1.15 (m, 45H). ¹³C NMR (151 MHz, CDCl₃) δ: 174.31, 174.02, 144.95, 144.39, 123.50, 98.07, 72.12, 70.58, 70.53, 70.49, 70.45, 69.51, 69.49, 69.06, 65.97, 64.99, 63.79, 63.62, 50.69, 50.16, 50.12, 48.36, 48.31, 41.87, 30.89, 24.60, 22.75, 18.68, 17.93. MS (MALDI-TOF MS, positive mode): calculated for C₂₃H₃₇N₄₅O₉₀: [M]⁺ *m/z* = 5221.62. Found: [M + Na]⁺ *m/z* = 5246.32.

Synthesis of the Triacylene Core. 1,1,1-Tris(hydroxymethyl)-propane (90.29 mg, 0.67 mmol) in 4 mL of dry DMF was placed in a flame-dried flask, and NaH (62.9 mg, 2.62 mmol) was added to the flask at 0 °C. After no further bubble evolution was observed, 503 mg of propargyl bromide (80 wt % toluene, 3.41 mmol) was added. The reaction was kept at 0 °C for 1 h and at RT for 5 h. The process was stopped at 0 °C using 7 mL of 1 M HCl and then extracted with EtOAc (3 × 15 mL). The crude product was purified by flash chromatography eluting with EtOAc/hexane (33/67, v/v) to give 132 mg (79%) of yellowish oily product. $T_g = -74.3$ °C. ¹H NMR (600 MHz, CDCl₃) δ: 3.41 (s, 6H), 2.40 (t, $J = 2.4$ Hz, 3H), 1.42 (q, $J = 7.6$ Hz, 2H), 0.88 (t, $J = 7.6$ Hz, 3H). ¹³C NMR (151 MHz, CDCl₃) δ: 80.16, 77.25, 77.04, 76.83, 74.02, 70.30, 58.63, 42.76, 22.71, 7.52, 7.50.

Synthesis of Dendrimer-[G1], D-[G1]. A flask, sealed with a rubber septum, was charged with N₃-[G1] (197.74 mg, 0.19 mmol) in 1.0 mL of DMF and 14.4 mg of triacetylene core in 733 μ L of DMF from a stock solution. The reaction system was degassed by three freeze–pump–thaw cycles and backfilled with argon. Then, CuBr (105 mg, 0.72 mmol) was added under argon followed by PMDETA addition (126 mg, 0.73 mmol) with an argon-purged syringe through the septum. Two freeze–pump–thaw cycles were performed to degas the system. The reaction mixture was stirred under argon atmosphere at RT. After reaction completion was verified by TLC, the organic phase was washed twice with brine to extract the copper catalyst. The solvent was evaporated, and the crude product was purified using flash chromatography eluting with methanol/EtOAc (25/75, v/v). Colorless oil (151 mg, 72%) was obtained after the evaporation of the solvent. $T_g = -7.5$ °C. ¹H NMR (600 MHz, CDCl₃) δ : 7.70 (s, 9H), 4.60 (s, 18H), 4.55–4.53 (m, 18H), 4.36–4.28 (m, 12H), 4.26–4.22 (m, 6H), 4.21 (d, $J = 11.8$ Hz, 12H), 3.91–3.88 (m, 18H), 3.73–3.57 (m, 80H), 1.43 (s, 18H), 1.37 (s, 18H), 1.24–1.15 (m, 29H), 0.75 (t, $J = 7.5$ Hz, 3H). ¹³C NMR (151 MHz, CDCl₃) δ : 174.21, 174.12, 145.30, 144.93, 123.57, 123.48, 98.05, 77.27, 77.06, 76.85, 72.10, 70.63, 70.55, 70.50, 70.46, 70.44, 69.49, 69.04, 65.95, 64.96, 64.90, 63.78, 63.60, 50.14, 50.08, 48.28, 43.13, 41.85, 24.63, 22.68, 18.65, 17.91, 7.59. MS (MALDI-TOF MS, positive mode): calculated for C₁₃₂H₂₂₁N₂₇O₅₇ [M]⁺ m/z = 3096.52. Found: [M + Na]⁺ m/z = 3119.489.

Synthesis of Dendrimer-[G2], D-[G2]. A flask sealed with a rubber septum was charged with N₃-[G2] (246.71 mg, 0.10 mmol) in 1.0 mL of DMF and 7.07 mg of triacetylene core in 621 μ L of DMF from a stock solution. The reaction system was degassed by three freeze–pump–thaw cycles and backfilled with argon. Then, CuBr (91 mg, 0.63 mmol) was added under argon, and PMDETA was added (106 mg, 0.62 mmol) with an argon-purged syringe through the septum. Two freeze–pump–thaw cycles were performed, and the reaction mixture was stirred at RT under argon. After completion, the organic phase was washed twice with brine. The solvent was evaporated, and the crude product was purified by flash chromatography with methanol/EtOAc (29/81, v/v) as eluent. Colorless oil (147 mg, 67%) was obtained after the solvent removal. $T_g = -6.2$ °C. ¹H NMR (600 MHz, CDCl₃) δ : 7.70 (s, 21H), 4.64–4.56 (m, 42H), 4.55–4.53 (m, 42H), 4.36–4.28 (m, 24H), 4.26–4.22 (m, 18H), 4.21 (d, $J = 11.8$ Hz, 23H), 3.91–3.88 (m, 42H), 3.73–3.57 (m, 198H), 1.45 (s, 36H), 1.39 (s, 36H), 1.24–1.15 (m, 63H). ¹³C NMR (151 MHz, CDCl₃) δ : 174.22, 174.14, 144.96, 123.58, 98.07, 72.12, 70.58, 70.53, 70.49, 70.45, 69.51, 69.06, 65.97, 64.99, 63.79, 63.62, 50.16, 50.12, 48.31, 41.87, 24.61, 22.75, 18.68, 17.93. MS (MALDI-TOF MS, positive mode): calculated for C₃₃₆H₅₄₅N₆₃O₁₂₉ [M]⁺ m/z = 7529.81. Found: [M + Na]⁺ m/z = 7554.

Synthesis of Dendrimer-[G3], D-[G3]. A dried flask was charged with N₃-[G3] (284 mg, 0.054 mmol) in 600 μ L of DMF and 3.76 mg of triacetylene core in 581 μ L of DMF from a stock solution. The reaction system, equipped with rubber septum, was degassed by three freeze–pump–thaw cycles and backfilled with argon. Then, CuBr (41 mg, 0.28 mmol) and PMDETA (47 mg, 0.27 mmol) were consecutively added under argon. Two freeze–pump–thaw cycles were performed to degas the system, and the reaction was stirred at RT under argon. After reaction completion, the crude product was purified by flash chromatography using methanol/EtOAc (50/50, v/v) as eluent and oily product (154 mg, 64%) was obtained. $T_g = -4.9$ °C. ¹H NMR (600 MHz, CDCl₃) δ : 7.71 (s, 45H), 4.62–4.61 (m, 90H), 4.55–4.53 (m, 90H), 4.35–4.28 (m, 48H), 4.25–4.22 (m, 42H), 4.21 (d, $J = 11.8$ Hz, 48H), 3.91–3.88 (m, 90H), 3.73–3.56 (m, 413H), 1.45 (s, 72H), 1.39 (s, 72H), 1.23–1.18 (m, 135H). ¹³C NMR (151 MHz, CDCl₃) δ : 174.22, 174.14, 144.96, 123.58, 98.07, 72.12, 70.58, 70.52, 70.49, 70.45, 69.51, 69.49, 69.06, 65.97, 64.99, 63.79, 63.62, 50.17, 50.12, 48.30, 41.87, 24.63, 22.74, 18.68, 17.94. MS (MALDI-TOF MS, positive mode): calculated for C₇₀₈H₁₁₄₅N₁₃₅O₂₇₃ [M]⁺ m/z = 15 912.00. Found: [M]⁺ m/z = 15 804.

General Procedure for the Deprotection of Dendrimer Peripheral Acetal Groups. The peripheral acetal groups were easily deprotected with TFA. Dendrimers were dissolved in a mixture of DCM/MeOH/TFA (40/40/20, v/v/v) and stirred for 2 h at RT. The solvent and excess of TFA were removed in a vacuum to afford hydroxyl-terminated dendrimers in high yield. The purity of the compounds after

deprotection was confirmed by ¹H NMR, ¹³C NMR, and MALDI-TOF MS.

D-[G1](OH)₁₂. ¹H NMR (600 MHz, DMSO) δ : 8.00 (s, 6H), 8.00 (s, 3H), 4.57–4.46 (m, 30H), 4.44 (s, 6H), 4.11–4.07 (m, 18H), 3.88–3.77 (m, 18H), 3.61–3.54 (m, 18H), 3.53–3.47 (m, 82H), 3.45 (d, $J = 5.6$ Hz, 8H), 1.25 (q, $J = 7.4$ Hz, 2H), 1.07 (s, 9H), 1.05 (s, 18H), 0.67 (t, $J = 7.5$ Hz, 3H). ¹H NMR (600 MHz, D₂O) δ : 8.07 (s, 6H), 8.05 (s, 3H), 4.64 (m, 30H), 4.55 (s, 6H), 4.33–4.25 (m, 12H), 4.23–4.18 (m, 6H), 3.99 (t, $J = 4.8$ Hz, 12H), 3.95 (t, $J = 4.8$ Hz, 6H), 3.78 (d, $J = 11.3$ Hz, 12H), 3.76–3.72 (m, 12H), 3.71–3.55 (m, 84H), 1.26 (q, $J = 7.1$ Hz, 2H), 1.20 (s, 9H), 1.17 (s, 18H), 0.66 (t, $J = 7.4$ Hz, 3H). ¹³C NMR (151 MHz, DMSO) δ : 174.54, 143.51, 124.11, 71.73, 69.67, 69.50, 68.68, 68.26, 64.03, 63.79, 63.04, 50.14, 49.30, 47.81, 39.94, 39.80, 39.66, 39.52, 39.38, 39.24, 39.10, 17.49, 16.79. MS (MALDI-TOF MS, positive mode): calculated for C₁₃₂H₂₂₁N₂₇O₅₇ [M]⁺ m/z = 3096.52. Found: [M + Na]⁺ m/z = 3119.489.

D-[G2](OH)₂₄. ¹H NMR (600 MHz, DMSO) δ : 8.00 (s, 12H), 8.00 (s, 9H), 4.56–4.45 (m, 78H), 4.44 (s, 6H), 4.23–4.03 (m, 42H), 3.89–3.77 (m, 42H), 3.66–3.35 (m, 240H), 1.25 (q, $J = 14.5$, 7.2 Hz, 2H), 1.11–0.98 (m, 63H), 0.66 (q, $J = 7.5$ Hz, 3H). ¹H NMR (600 MHz, D₂O) δ : 8.07 (d, $J = 9.0$ Hz, 12H), 8.05 (s, 9H), 4.67–4.56 (m, 78H), 4.53 (s, 6H), 4.30–4.23 (m, 24H), 4.20–4.17 (m, 18H), 4.00–3.89 (m, 42H), 3.76 (t, $J = 10.3$ Hz, 24H), 3.74–3.69 (m, 24H), 3.69–3.55 (m, 192H), 1.24 (q, $J = 7.1$ Hz, 2H), 1.18 (s, 36H), 1.16 (s, 18H), 1.13 (s, 9H), 0.63 (t, $J = 7.5$ Hz, 3H). MS (MALDI-TOF MS, positive mode): calculated for C₃₀₀H₄₉₇N₆₃O₁₂₉ [M]⁺ m/z = 7046.43. Found: [M + Na]⁺ m/z = 7078.93.

D-[G3](OH)₄₈. ¹H NMR (600 MHz, DMSO) δ : 8.00 (s, 24H), 8.00 (s, 21H), 4.53–4.46 (m, 174H), 4.44 (s, 6H), 4.24–4.02 (m, 90H), 3.89–3.76 (m, 90H), 3.63–3.40 (m, 510H), 1.14–0.97 (m, 135H), 0.66 (t, $J = 7.4$ Hz, 3H). ¹H NMR (600 MHz, D₂O) δ : 8.07 (s, 24H), 8.05 (s, 12H), 8.04 (s, 9H), 4.66–4.54 (m, 174H), 4.52 (s, 6H), 4.25–4.24 (m, 48H), 4.18–4.14 (m, 42H), 4.00–3.94 (m, 48H), 3.93–3.86 (m, 12H), 3.75 (d, $J = 11.2$ Hz, 48H), 3.73–3.68 (m, 48H), 3.68–3.51 (m, 438H), 1.16 (s, 72H), 1.14 (s, 36H), 1.12 (s, 18H), 1.11 (s, 9H), 0.61 (t, $J = 7.5$ Hz, 3H). ¹³C NMR (151 MHz, DMSO) δ : 174.58, 173.45, 143.62, 124.08, 71.72, 69.67, 69.50, 68.68, 68.26, 68.13, 67.40, 64.03, 63.81, 63.25, 63.05, 50.15, 49.30, 47.81, 46.18, 43.61, 39.94, 39.80, 39.66, 39.52, 39.38, 39.24, 39.10, 17.49, 17.06, 16.80. MS (MALDI-TOF MS, positive mode): calculated for C₆₃₆H₁₀₄₉N₁₃₅O₂₇₃ [M]⁺ m/z = 14 946.24. Found: [M]⁺ m/z = 14 952.66.

The geometry optimizations of the model bis-MPA compound for the dendrimer branching site and its complex with palladium(II) were performed using density functional theory (DFT),²³ employing the Becke 3-parameter Lee–Yang–Parr (B3LYP) functional.²⁴ LAN2DZ pseudopotential²⁵ was utilized to model the palladium(II) ions, while the 6-31G(d) basis set²⁶ was chosen for all remaining elements. The geometry minima were confirmed by frequency analysis, and zero point vibrational energy (ZPVE) was included in the results for energies. All calculations were performed with the Gaussian 09 program.²⁷

General Procedure for Palladium Complexation on Dendrimers. Acetal- or hydroxyl-terminated dendrons or dendrimers were dissolved in DMSO followed by adding 3 equiv of Pd(PhCN)₂Cl₂ according to the number of potential chelating sites. The complexation was conducted at RT under argon and is complete within 5 min as monitored by ¹H NMR. The excess of Pd(PhCN)₂Cl₂ was isolated by cold filtration and washed with cold CHCl₃. The products were obtained by removing the solvent under vacuum. An example is shown below.

Cl-[G1]-PdCl₂, Cl-[G1]. Cl-[G1] (24.73 mg, 0.024 mmol) and Pd(PhCN)₂Cl₂ (25.68 mg, 0.067 mmol) were dissolved in 2 mL of CH₃CN (or DMSO) under argon. The reaction solution was stirred at 30 °C for 1 h. The excess of Pd(PhCN)₂Cl₂ was removed by cold filtration and washed with cold CHCl₃. A yellowish oil (24 mg, 84%) was obtained by removing the solvent under vacuum. ¹H NMR (600 MHz, CDCl₃) δ : 7.74 (s, 2H), 5.01 (d, $J = 11.4$ Hz, 2H), 4.88 (d, $J = 11.4$ Hz, 2H), 4.57 (t, $J = 4.6$ Hz, 4H), 4.38 (d, $J = 8.4$ Hz, 2H), 4.33–4.30 (m, 6H), 4.23–4.16 (m, 6H), 3.87 (t, $J = 4.7$ Hz, 4H), 3.77 (t, $J = 5.8$ Hz, 2H), 3.7 (t, $J = 4.8$ Hz, 2H), 3.72–3.55 (m, 20H), 1.44 (s, 6H), 1.39 (s, 6H), 1.32 (s, 3H), 1.20 (s, 6H). ¹³C NMR (151 MHz, CDCl₃) δ : 174.67, 174.17, 145.94, 125.14, 98.08, 71.86, 71.41, 70.69, 70.65, 70.57, 70.33, 69.15, 69.09,

68.70, 65.99, 63.79, 62.54, 51.83, 47.84, 42.86, 41.91, 24.91, 22.46, 19.29, 18.66. ^1H NMR (600 MHz, DMSO) δ : 8.26 (s, 2H), 4.87 (d, J = 11.3 Hz, 2H), 4.80 (d, J = 11.3 Hz, 2H), 4.64–4.57 (t, J = 4.8 Hz, 4H), 4.25–4.13 (m, 6H), 4.06–4.01 (m, 6H), 3.84 (t, J = 5.0 Hz, 4H), 3.74–3.37 (m, 28H), 1.35 (s, 6H), 1.25 (s, 6H), 1.20 (s, 3H), 1.07 (s, 6H).

Stock Solution of D-[G1](OH)₁₂(PdCl₂)₃. A stock solution of palladium complex was made by dissolving 5.7 mg of waxy D-[G1](OH)₁₂(PdCl₂)₃ in 1 mL of DI H₂O. After being filtered through a 0.2 μm PVDF membrane, part of the solution was further diluted 30 times for the ICP-MS measurement. The palladium concentration of the diluted solution was measured to be 3.0 ppm.

Suzuki–Miyaura Coupling Reaction. 5 mL of conical reaction vial was charged with 4-bromoacetophenone (48.42 mg, 0.24 mmol), phenylboronic acid (45.49 mg, 0.37 mmol), triethylamine (49.22 mg, 0.49 mmol), and 800 μL of H₂O. The appropriate amount of D-[G1](OH)₁₂(PdCl₂)₃ stock solution (0.02 mol %) was withdrawn and added to the mixture. The reaction mixture was kept at 60 °C for 3 h. After completion, the product was extracted with ethyl acetate (3 \times 7 mL). The combined organic layer was dried over MgSO₄, and the solvent was removed under vacuum to give solid white crystals as product (43.82 mg, 100%). The identification of the product was conducted by 300 MHz NMR. ^1H NMR (300 MHz, CDCl₃) δ : 8.04 (d, J = 8.7 Hz, 2H), 7.69 (d, J = 8.7 Hz, 2H), 7.63 (d, J = 6.9 Hz, 2H), 7.53–7.44 (m, 2H), 7.42 (dd, J = 5.0, 3.6 Hz, 1H), 2.64 (s, 3H). ^{13}C NMR (75 MHz, CDCl₃) δ : 197.79, 145.89, 140.00, 136.02, 129.07, 129.02, 128.34, 127.38, 127.33, 26.74.

RESULTS AND DISCUSSION

The strategic goal of this study was to develop and produce a dendrimer which could be employed in a broad array of functions—from “green” chemistry to biomedical. Two key design elements were considered at the planning stage: (a) intrinsic water solubility at the periphery and throughout the interior of the macromolecule and (b) potential hydrolysability of the entire dendritic framework. The building block, chosen to meet the first (a) requirement was triethylene glycol, TrEG, a low molecular weight member of the poly(oxyethylene) family. This polymer, also known as poly(ethylene glycol), PEG, or poly(ethylene oxide), PEO, has long been known for its versatility and wide-ranging applications.²⁸ PEGylation was often used to

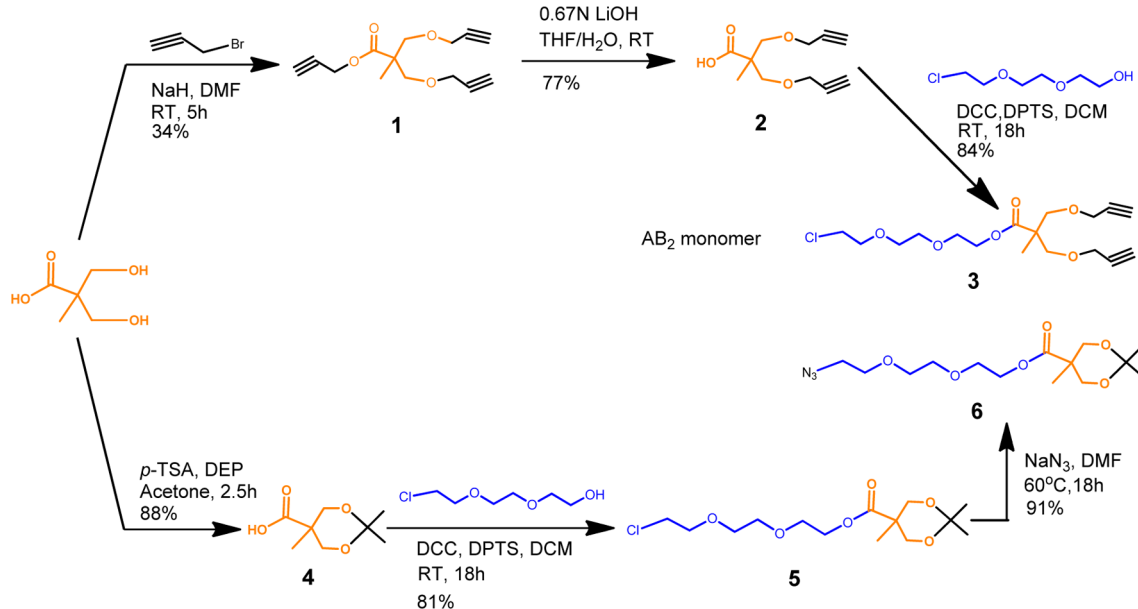
modify dendritic periphery for specific applications,^{21,29} but PEGs or PEOs have been much less frequently used as interior building blocks of dendrimers.³⁰ TrEG is expected to provide water solubility and flexibility of the branches, while still preserving certain size selectivity of the dendritic interior. The readily available 2,2-bis(hydroxymethyl)propionic acid, bis-MPA, was considered suitable compound to meet requirement b and was used as the parent branching fragment because of its versatility in dendrimer synthesis³¹ and potential biodegradability and biocompatibility.³²

The synthetic strategy for the AB₂ monomer is depicted in Scheme 1. A bis-alkyne-modified bis-MPA derivative (**2**) is synthesized via Williamson ether synthesis. Unfortunately, the reaction proceeds through intermediate **1**, produced in low yield of 34%, and an extra hydrolysis is required to obtain **2**. This particular step could be considered as the yield-determining reaction of the entire synthetic procedure. A chlorinated derivative of TrEG, 2-[2-(2-chloroethoxy)ethoxy]ethanol, is then attached as a short spacer to **2** via DCC-mediated esterification reaction affording the AB₂ ether–ester monomer **3**.

A complementary azide derivative of bis-MPA **6** was synthesized by DCC coupling of the same 2-[2-(2-chloroethoxy)ethoxy]ethanol with acetyl protected bis-MPA, followed by converting the ~CH₂Cl end group into the corresponding azide (**6**, Scheme 1). Azide **6** is a structural analogue of the AB₂ monomer and serves as the starting reagent in the convergent synthetic scheme. It also provides the opportunity to cover the dendrimer periphery with terminal hydroxyl groups, which are created and available for further modification after a simple deprotection process.

The convergent method, employed in the new dendrimer synthesis, is shown in Scheme 2. The dendron growth proceeds by “click” reaction of the AB₂ monomer **3** with slight stoichiometric excess (1.1 equiv) of azide segments **6**. The product is easily purified by column chromatography (see Experimental Section for separation conditions) due to the significant molecular weight difference between the starting reagents and the newly produced macromolecules. In this way dendrons up to third generation are successfully synthesized with

Scheme 1. Synthesis of AB₂ Monomer and Complementary Azide



relatively high yields and high structural purity as evidenced by SEC (Figure 1), MALDI-TOF (Figure 2), and NMR analyses (Figure 3).

The SEC traces of chloro-dendrons Cl-[G1]–Cl-[G3] (Figure 1) reveal traditionally monomodal and sharp peaks with the polydispersity indices (PDIs) varying from 1.01 to 1.03. As expected, the apparent molecular masses, calculated by conventional calibration, increasingly deviate from the expected theoretical values (Table 1). The SEC analyses of the azide derivatives show a similar trend. Convincing evidence for the high purity and structural integrity of the dendrons formed is

Table 1. Molecular Mass Characteristics of Dendrons Cl-[G1]–Cl-[G3] Obtained by SEC Using Conventional Calibration

dendron	theor mass	SEC (THF) ^a			
		M_n	M_w	M_p^b	M_w/M_n
Cl-[G1]	1022	750	760	770	1.01
Cl-[G2]	2419	1710	1760	1810	1.03
Cl-[G3]	5212	3810	3880	3960	1.02

^aPSt standards were used. ^b M_p is the apparent molecular mass at the peak maximum.

Scheme 2. Convergent Growth of Dendrons

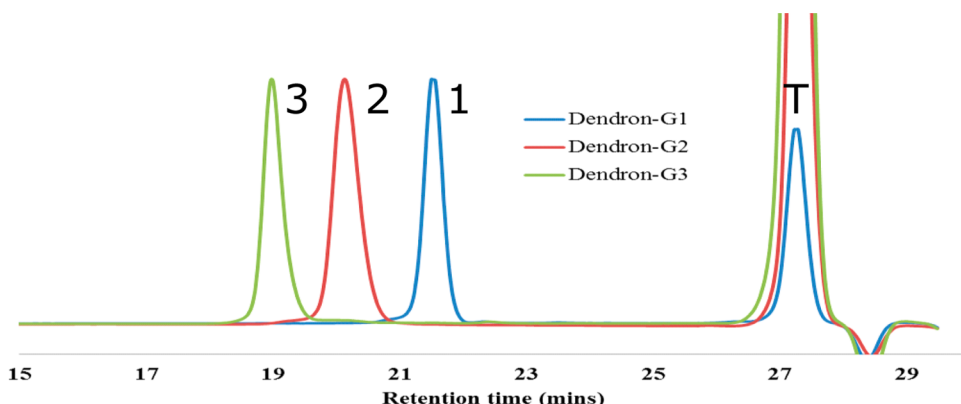
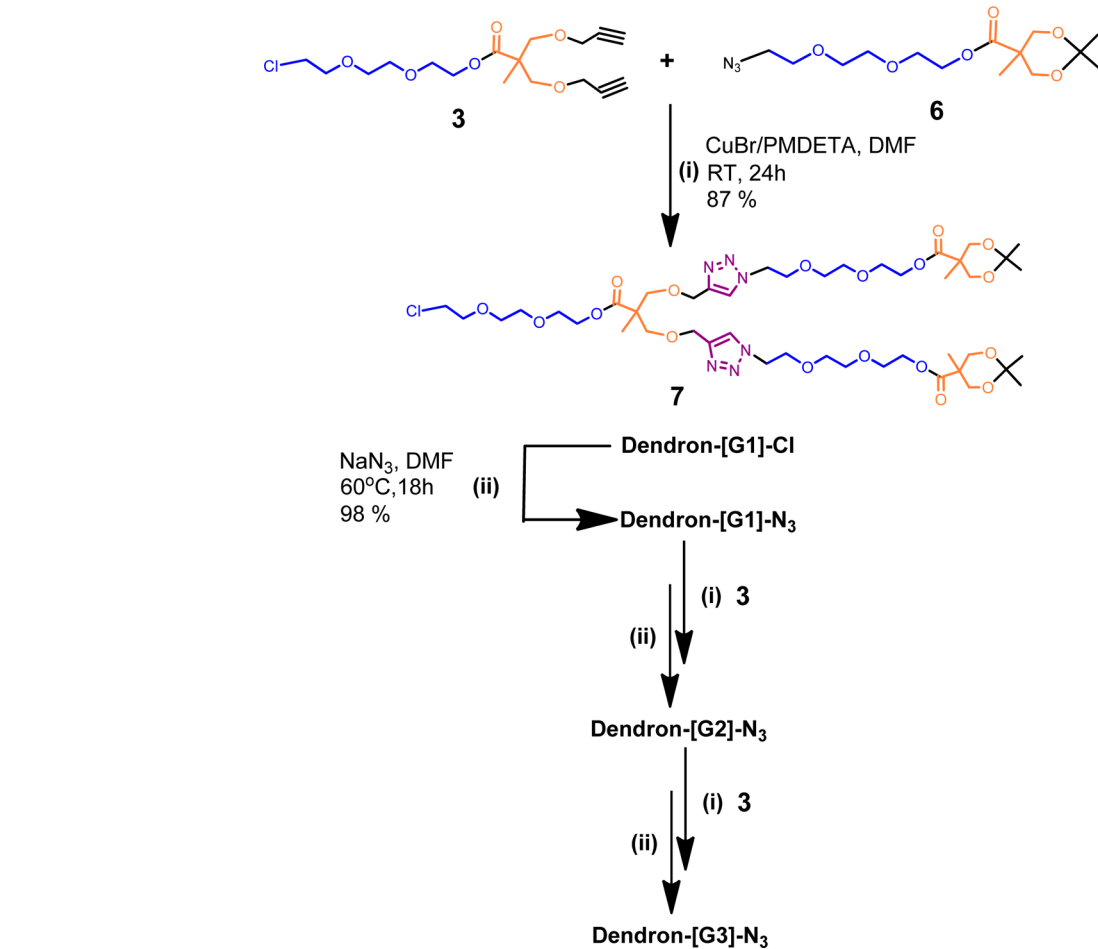


Figure 1. SEC traces (THF, dRI detector) of (1) Cl-[G1], blue trace, (2) Cl-[G2], red trace, and (3) Cl-[G3], green trace. (T) Toluene: an internal standard.

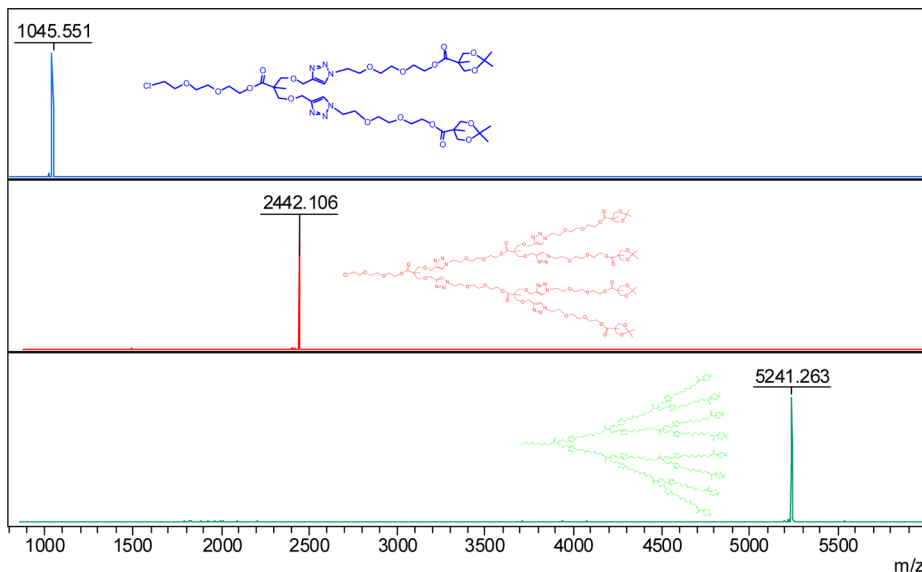


Figure 2. MALDI-TOF spectra of Cl-[G1], blue trace, $[M + Na]^+ = 1045.551$; Cl-[G2], red trace, $[M + Na]^+ = 2442.106$, and Cl-[G3], green trace, $[M + Na]^+ = 5241.263$.

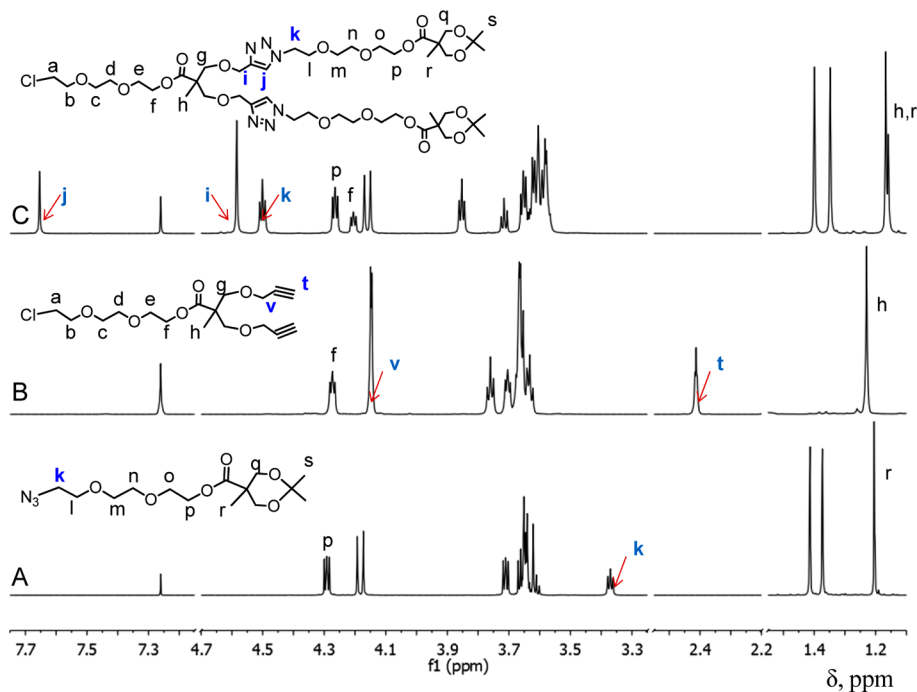


Figure 3. 600 MHz ^1H NMR spectra of 6 (A), 3 (B), and Cl-[G1] (C), recorded in CDCl_3 at 298 K.

provided by the MALDI-TOF analyses (Figure 2), where single molecular ion $[M + \text{Na}]^+$ peaks are observed in the spectra and molecular masses matching the theoretical ones.

The chemical composition of the dendrons formed is confirmed by NMR analyses (Figure 3). The acetylene protons in 3 (t, Figure 3B) disappear. The signals for the methylene protons next to the azide group in 6 (k, Figure 3A) and the methylene protons adjacent to the acetylene group in 3 (v, Figure 3B) shift downfield (Figure 3C, k and i, respectively). The formation of the triazole ring and the preservation of ester linkages during the synthetic sequence are also proven by NMR analyses: triazole protons (j, Figure 3C) appear as clean singlets at 7.0 ppm; the methylene protons adjacent to the triazole rings (i and k, Figure 3C) are visible at 4.63 and 4.55 ppm, respectively,

and the ester methylene protons (f and p, Figure 3C) show as triplets at 4.21 and 4.25 ppm, respectively. All signals have been further identified by full COSY assignments. An example is shown in Figure 4, where the several pairs of structural protons are highlighted: k and l, p and o, q and q. Finally, the structural and chemical purity of the dendrons is independently confirmed by the integral intensity ratios of the TrEG end group protons and the triazole protons. An example with dendrons [G1]-N3-[G3]-N3 is shown in Figure 5.

In the final act of the synthetic sequence first-, second-, and third-generation dendrimers are constructed by connecting azide-terminated dendrons to a triacetylene core using the same type of “click” chemistry. A 1.2 stoichiometric excess of the corresponding dendron is employed, and the reaction is

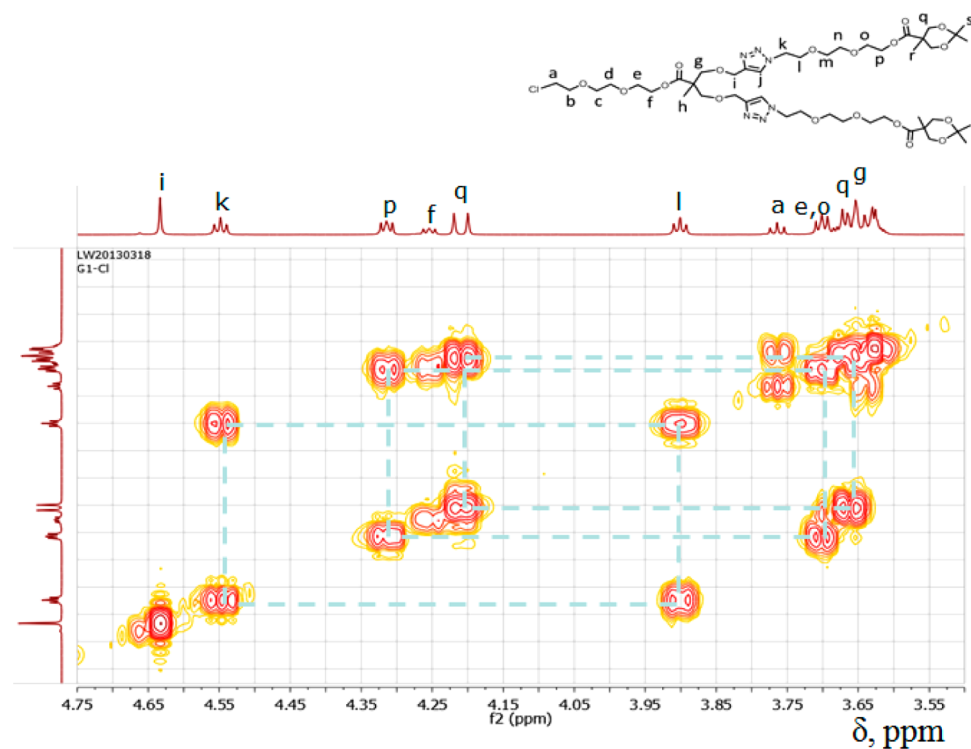


Figure 4. 600 MHz ^1H NMR ge-COSY spectra of Cl-[G1], recorded in CDCl_3 at 298 K.

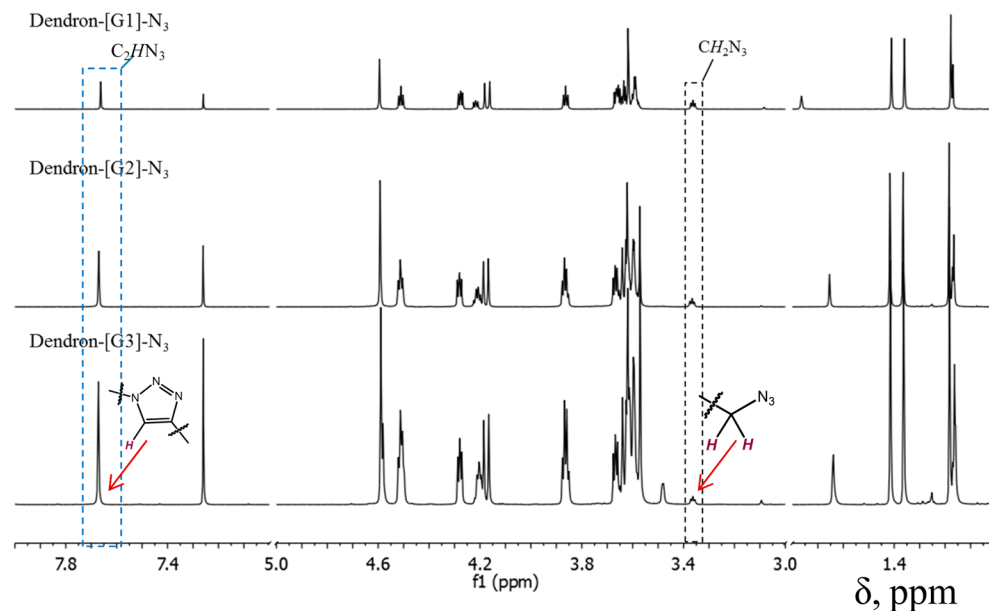


Figure 5. 600 MHz ^1H NMR overlay of $\text{N}_3\text{-}[\text{Gn}]$ dendrons recorded in CDCl_3 , 298 K.

performed at room temperature. It is worth mentioning that the short TrEG segments are seemingly reducing the steric congestion at the bond-forming event and facilitate the growth of dendrimers free of structural defects in relatively high yields: 72% for D-[G1], 67% for D-[G2], and 64% for D-[G3]. The azide dendron “click” coupling to the triacetylene core is monitored by SEC (Figure 6). It is evident that the process could proceed to completion even when relatively large dendrons (molecular mass >5000 Da) are involved. At this time we cannot explain the appearance of the higher molecular mass shoulder in peak 2 (Figure 6, 16.7 min).

The chemical structure of all dendrimers is characterized by NMR. An example for hydroxyl-coated dendrimers is shown in Figure 7 (for an example of 2D ^1H - ^{13}C DEPT-HSQC NMR analysis see Figure S5 in the Supporting Information). An important feature of the layered structure, seen in dendrimers of generations higher than 1, is the differentiating in the proton chemical shifts at the branching sites. Indeed, the same trend is clearly evident in the newly produced macromolecules: the bis-MPA methyl protons show different chemical shifts in the range between 1.04 and 1.12 ppm for the three different generations. More importantly, the peak deconvolution of the signals for the triazole protons (7.95–7.99 ppm) also demonstrates the

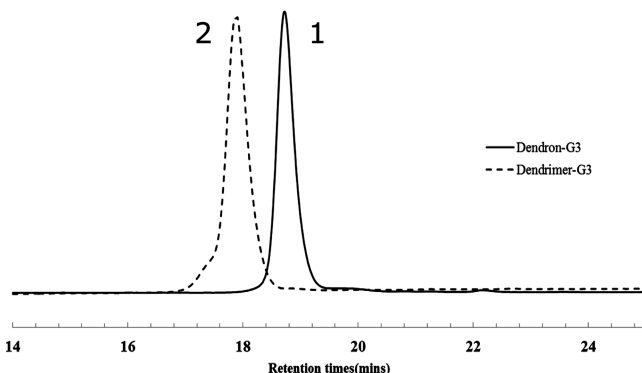


Figure 6. SEC traces of $\text{N}_3\text{-[G3]}$ (1) and dendrimer D-[G3] (2).

increasingly reduced local mobility in the layers from the periphery to the core even for groups not in the immediate vicinity of the branch (Figure 7). The molecular mass and structural uniformity of the dendritic macromolecules are further verified by SEC and MALDI-TOF (Figure 8a,b), respectively. Interestingly, dendrimer D-[G1] appears to have well-pronounced low molecular mass tail in the SEC chromatogram (Figure 8a, 1) but shows as a single peak, perfectly matching the theoretical molecular mass in the MALDI-TOF spectrum (Figure 8b, 1).

We believe that this is due to the extended low-molecular-mass resolution capacity of the SEC column set, used for the analysis.³³ On the opposite, dendrimer D-[G3] is seen as single peak in the chromatography analysis but appears as a broad poorly resolved peak in the MALDI-TOF traces regardless of the matrix and analysis conditions used (Figure 8b). The failure of the mass spectrometric analysis to confirm the structural purity and uniformity of D-[G3] is certainly regrettable, but similar broadening is not uncommon for dendrimers of this size and

chemical composition.³⁴ The small broad peak around 11 kDa is probably caused by partial fragmentation of the dendrimer due to the increased laser beam attenuation, required to volatize the macromolecule. The structural homogeneity of the third-generation dendrimer is independently confirmed by DLS, another size-sensitive technique (Figure 9). The sizes determined by this method (3.8, 6.4, and 11.5 nm for D-[G1](OH)₁₂, D-[G2](OH)₂₄, and D-[G3](OH)₄₈, respectively) are higher than the usually encountered values for dendrimer generations 1–3 and reflect the presence of the hydrophilic TrEG spacers throughout the dendritic skeleton.

The results obtained show that the synthetic strategy can successfully lead to defect-free third-generation dendrimers, which have 48 protected primary hydroxyl groups, 45 hydrolyzable ester linkages, and 21 potential metal-binding sites (Figure 10). These dendrimers are freely soluble in water, methanol, CH_2Cl_2 , CHCl_3 , CH_3CN , ethyl acetate, DMF, DMSO, THF, and other solvents, mostly due to the substantial presence of TrEG blocks—a total of 45 such fragments in D-[G3]. While these chemical functionalities and solution properties make the newly formed macromolecules intriguing candidates for biomedical applications, this study will explore *only* the chelating potential of the triazole moieties distributed across the dendrimer framework and the catalytic activity of dendritic Pd complexes in Suzuki–Miyaura reactions.

A model compound consisting of bis-MPA branching unit connected to two triazole rings via the primary hydroxyl groups is used to predict the most suitable location of the binding sites. Methyl groups attached to the N1 and N4 atoms in the triazole rings and the bis-MPA COO unit represent the links to the rest of the dendrimer (Figure 11a). The optimized geometry of the model compound is presented in Figure 11b. The Millikan atomic charges on the N1–N6 atoms in 1,2,3-triazole rings are calculated to be -0.235 , -0.094 , -0.350 , -0.218 , -0.083 , and -0.327 ,

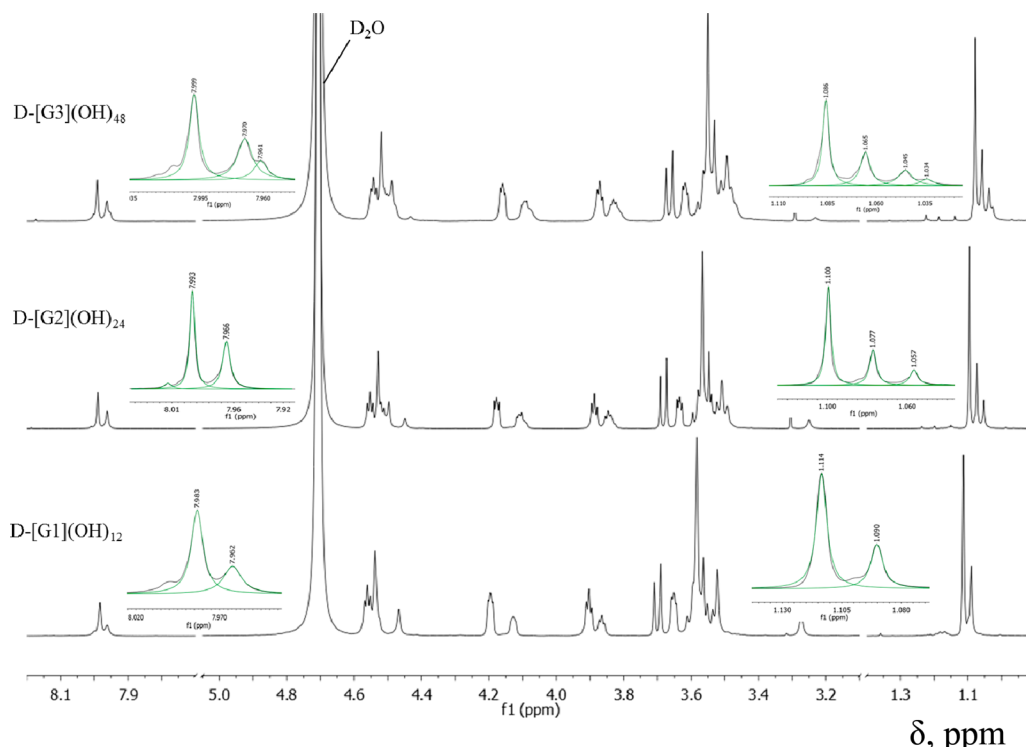


Figure 7. Overlay of 600 MHz ^1H NMR spectra of dendrimers D-[Gn](OH)_m recorded in D_2O , 298 K.

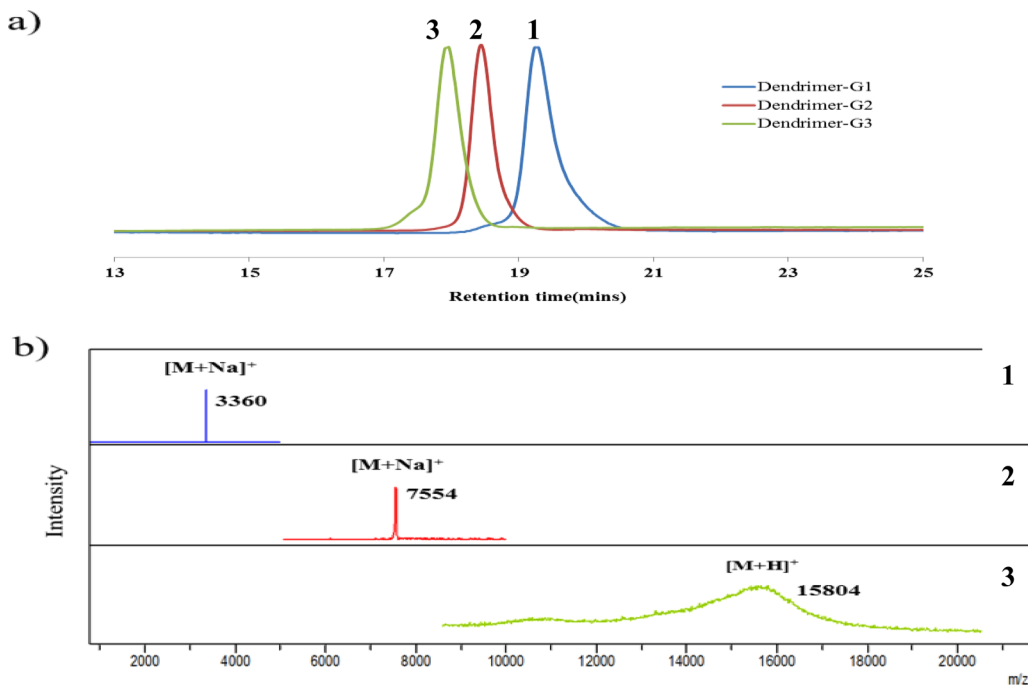


Figure 8. Chromatographic and mass spectrometric analyses of dendrimers D-[G1] (1), D-[G2] (2), and D-[G3] (3): (a) SEC traces; (b) MALDI-TOF spectra.

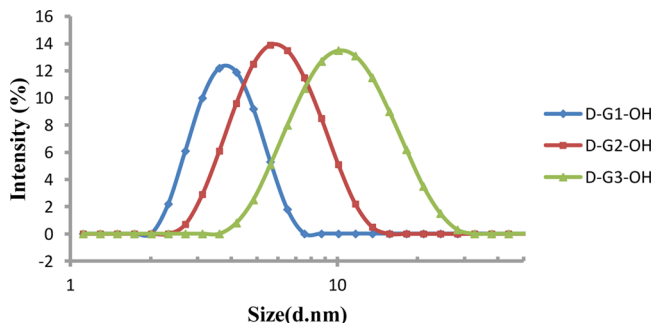


Figure 9. DLS traces of dendrimers D-[Gn](OH)_m in water.

respectively, indicating that N1/N4 and N3/N6 pairs are the most possible electron donors for the metal complexation.

The two coordination modes of N1–N4 and N3–N6 pairs in the two heterocycles are also evaluated in the model study. The results show that N3–N6 coordination is the most thermodynamically favorable since the Gibbs free energy of the reaction ($\Delta G^\circ_{298.15\text{ K}}$) is $-46.1\text{ kcal mol}^{-1}$ compared to $13.7\text{ kcal mol}^{-1}$ for N1–N4 coordination. As shown in Figure 12b, the geometry optimization of Pd(II) complex via N3/N6 coordination leads to a complex with square-planar geometry with the two triazoles forming a bidentate ligand in preferable *trans* position. In this way the theoretical models predict that a 12-membered ring would form as the chelate pocket at the branching sites in the dendrimer molecules.

The dendron Cl-[G1] was initially used as a model compound to investigate the possible coordination chemistry of the triazole “clefts” to palladium(II) by interaction with 3 mol equiv ($\text{Pd}(\text{PhCN})_2\text{Cl}_2$) in CH_3CN or DMSO. The binding in both solvents is fast and is complete within 5 min as revealed by ^1H NMR analysis *in situ*. The study is further extended to dendrimers of generations 1–3 with similar outcome. Remarkably, the data from the NMR analyses (^1H -, ge-COSY, and

DEPT-HSQC) show convincingly the formation of the chelate ring, postulated by the theoretical modeling. The spectrum of D-[G2] before and after the complexation is shown in Figure 13. The signals of several protons are shifted downfield, compared to those in the starting dendrimer, suggesting a deshielding process in result of changes in their architectural arrangement and appearance of electron-withdrawing groups (PdCl_2). For example, the triazole protons (Figure 13a, j) are probably facing inward in the starting dendrimer but facing outward after the heterocycles “flip” during the coordination process with PdCl_2 (Figure 13b). The reduced segmental mobility of the groups in the 12-membered ring leads to inequivalent surroundings and is manifested by transformation of the peaks due to methylene protons i and g from singlets at 4.55 and 3.5 ppm, respectively (Figure 12a), into doublets of doublets (Figure 13b). Both NMR and ICP-MS analyses show that the complexation efficiency $95 \pm 5\%$ for all dendrimers, suggesting the formation of dendritic complexes with 3, 9, and 21 Pd moieties (for generations 1, 2, and 3, respectively).

The incorporation of multiple PdCl_2 groups and the formation of multiple rings throughout the dendritic macromolecules would most probably affect their size as well. Indeed, both DLS and TEM analyses confirm this assumption. The increases in the hydrodynamic diameter of the dendrimers D-[G1], D-[G2], and D-[G3] after the complexation are evident in the DLS traces shown in Figure 14. It should also be noted that the mixture $\text{CH}_3\text{CN}/\text{H}_2\text{O}$ is not as good solvent as pure water, and the dendrimers sizes shrink from 3.8, 6.4, and 11.5 nm to 3.0, 4.9, and 7.2 nm for D-[G1](OH)₁₂, D-[G2](OH)₂₄, and D-[G3](OH)₄₈, respectively (compare to Figure 9). All species, however, retain their monomodal size distribution during this process. The dendrimer size expansion after complexation amounts to 30% ($3.9 \pm 0.9\text{ nm}$), 49% ($7.3 \pm 0.5\text{ nm}$), and 117% ($15.6 \pm 0.2\text{ nm}$) for generations 1, 2, and 3, respectively, measured in the same $\text{CH}_3\text{CN}/\text{H}_2\text{O}$ solution. We believe that the size increase is predominantly caused by the incorporation of the voluminous

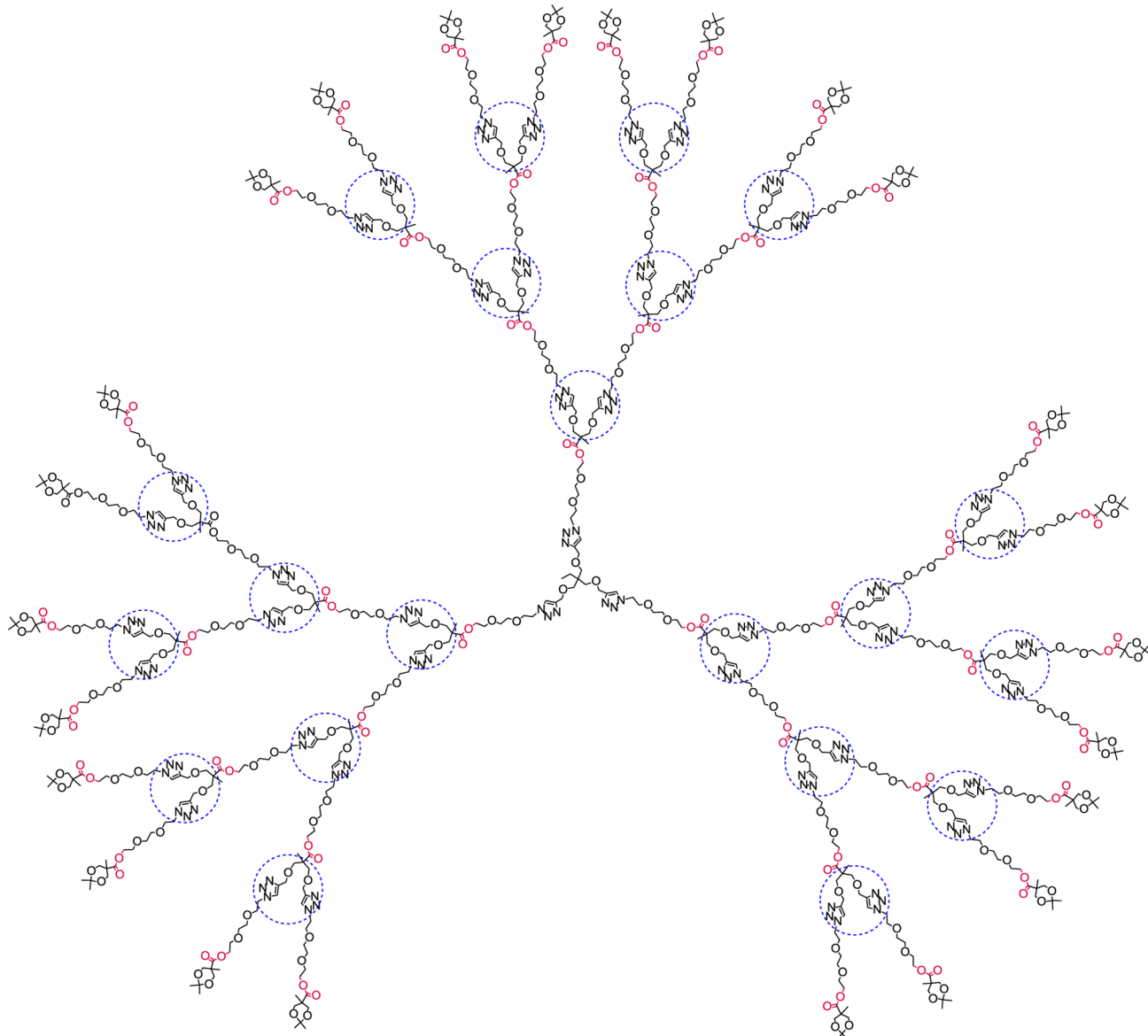


Figure 10. Chemical structure of dendrimer D-[G3]. The ester linkages are marked in magenta, and the potential binding sites are encircled.

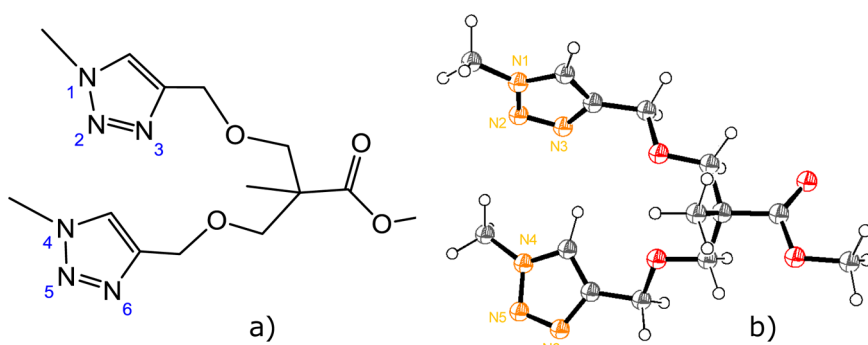


Figure 11. Chemical structure (a) and ORTEP diagram (b) of the model compound, representing the branching sites in the TrEG dendrimer. C atoms (gray spheres), H atoms (white spheres), N atoms (orange spheres), and O atoms (red spheres).

Pd moieties, but partial contribution of the increased osmotic pressure due to complex charges should also be taken into account. The notable broadening in the DLS trace of D-[G3]-Pd suggests a possible formation of aggregates, and complementary

TEM analyses hint at their presence (Figure 15). Compared with the hydrodynamic diameters of the empty D-[G3](OH)₄₈ (7.2 ± 0.2 nm) and Pd-loaded D-[G3](OH)₄₈(PdCl₂)₂₁ (15.6 ± 0.2 nm), the increased diameter size of the species observed by

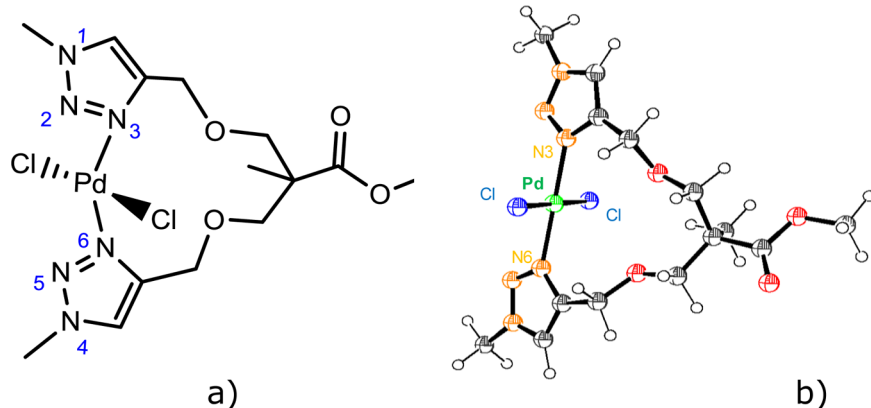


Figure 12. Chemical structure (a) and ORTEP diagram (b) of the palladium(II) complex for the model compound representing the metal-binding sites in the TrEG dendrimer. C atoms (gray spheres), H atoms (white spheres), N atoms (orange spheres), O atoms (red spheres), Cl atoms (blue spheres), and Pd atom (green sphere).

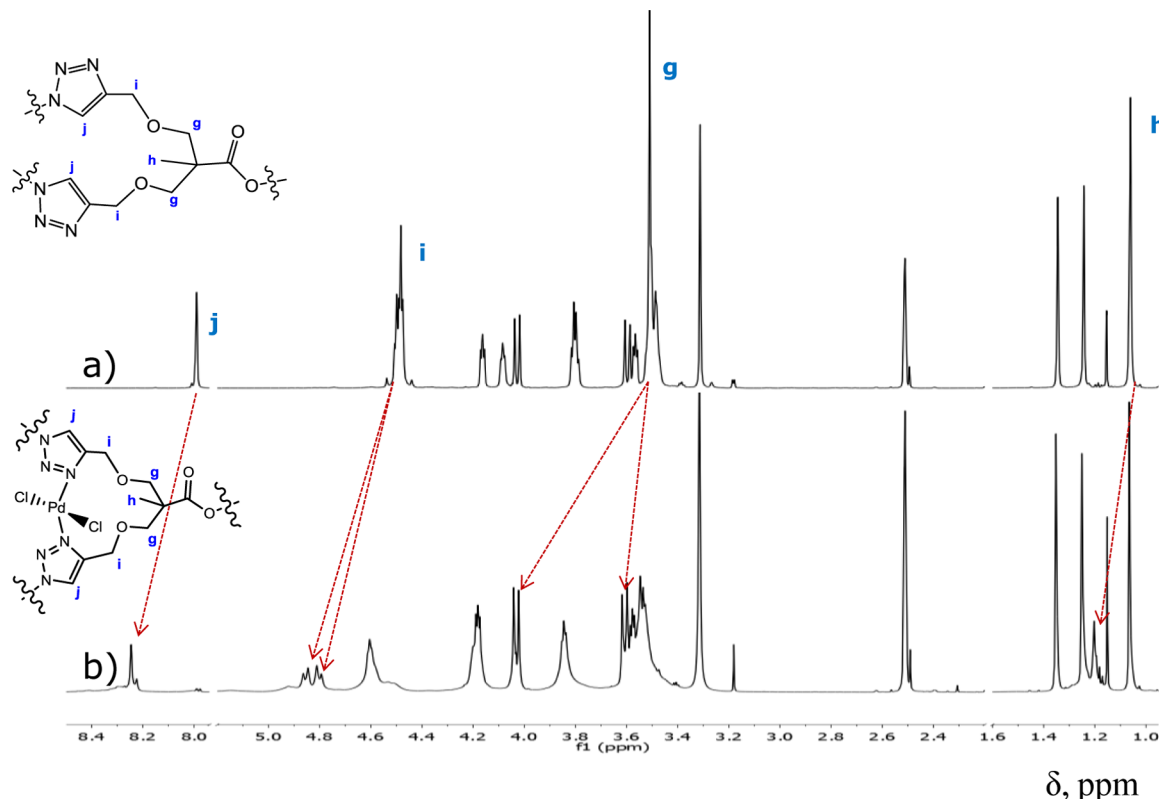
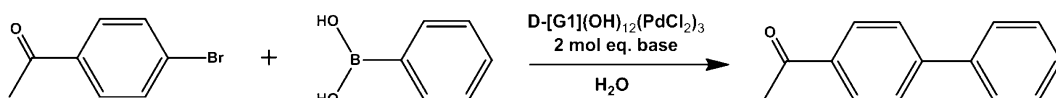


Figure 13. ¹H NMR spectra of (a) dendrimer D-[G2] and (b) palladium(II) complex of D-[G2]. Analysis conditions: 600 MHz, DMSO-*d*₆, 298 K.

Scheme 3. Suzuki–Miyaura Reaction Catalyzed by D-[G1](OH)₁₂(PdCl₂)₃



TEM (13.9 ± 1.8 and 23.9 ± 0.9 nm, respectively; see Figure S9 and Table S1) could only be partially attributed to the natural “flattening” of these soft nano-objects. On the other side, the careful examination of the TEM images of the dendrimers (Figure 15) shows several overlapping pairs of ovoid structures—an indication for a possible dimer aggregation.

The catalytic activity of the new dendritic palladium complexes for Suzuki–Miyaura reactions in water is evaluated by pilot

experiments with conventional reagents—phenylboronic acid and 4-bromoacetophenone (Scheme 3). The preliminary results show that with D-[G1](OH)₁₂(PdCl₂)₃ and triethylamine (Et₃N) as the base the conversion is quantitative at 100 °C. Further experiments show that lowering the reaction temperature to 60 °C does not affect the yield, which stays at 100%. When K₂CO₃ is used as base, quantitative yield could be achieved even at 50 °C (Table 2). Comparison to previously published results

Table 2. Suzuki–Miyaura Reaction between 4-Bromoacetophenone and Phenylboronic Acid, Catalyzed by Different Pd Complexes in Water^a

temp (°C)	Pd (mol %)	time (h)	yield (%)	ref
50	0.029	3	99	this work
60	0.01	3	92	35a
78	0.04	0.5	60	18g
80	0.00001–0.01	4–40	85–100	35b
90	0.1	2	94–96	36a
100	0.1	2	81–95	36b, c
100	0.001–0.01	1–3	94–99	37a
100	0.25	16	>99	37b
100	0.003	5	94–95	38a
100	0.1	8	95	38b
100	0.3	4–7.5	92–94	39
110	0.001–1.0	2–4	59–99	40
120	0.1	1	100	41

^aReaction conditions: [bromoacetophenone]:[phenylboronic acid]:[K₂CO₃] = 1:1.5:2 mol equiv.

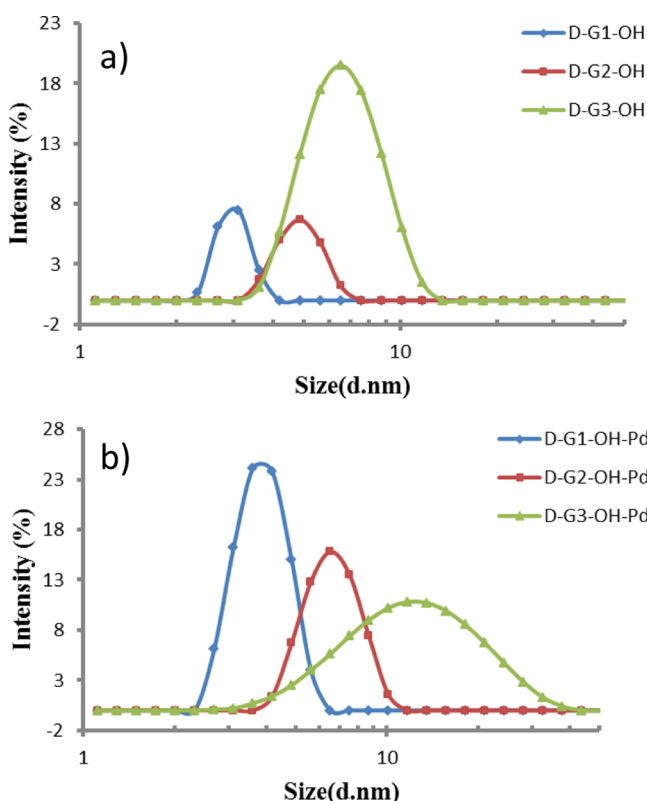


Figure 14. Hydrodynamic diameter of dendrimers before (a) and after (b) interaction with Pd(PhCN)₂Cl₂. DLS analysis in CH₃CN/H₂O (30/70, v/v).

for the reaction of the *same* reagents, in the *same* solvent (H₂O) and the *same* base (K₂CO₃), shows that the yields, achieved under these relatively mild conditions, place the new dendritic Pd complexes among the promising catalysts for this type of cross-coupling syntheses (Table 2). The Pd complexes of higher-generation dendrimers behave in a similar fashion (see Supporting Information). Currently more experiments are underway to establish the catalytic mechanism to evaluate the extent of Pd leaching and the applicability to other synthetically important reagents.

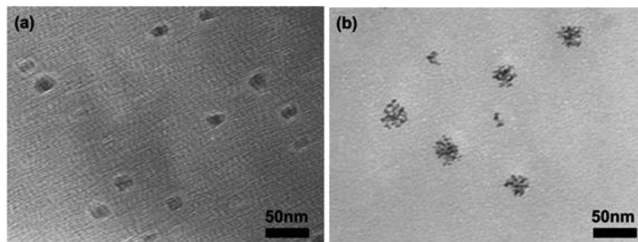


Figure 15. TEM micrographs of dendrimer D-[G3](OH)₄₈ before (a) and after (b) complexation with Pd(PhCN)₂Cl₂. Dendrimers deposited from CH₃CN/H₂O (30/70, v/v) solution.

CONCLUSIONS

In summary, we have synthesized a new class of poly(ether-ester) dendrimers with expandable and flexible hydrophilic triethylene glycol spacers and triazole rings at the ester branching sites. The materials range in size between 3 and 12 nm and are soluble in a broad variety of solvents. The excellent accessibility and binding ability of the triazole/bis-MPA branching sites were demonstrated by fast and quantitative formation of PdCl₂ complexes under mild reaction conditions, which in turn can quantitatively catalyze classic Suzuki–Miyaura cross-couplings in water. These results provide encouraging indication that the triazole poly(ether-ester) dendrimers might behave similarly toward other VIIIa group elements, which makes them suitable carriers of diverse functions from environmentally friendly catalysis to specific drug delivery. Our group is currently performing further experiments to validate this assumption.

ASSOCIATED CONTENT

Supporting Information

Additional experimental procedures, SEC and DSC traces, NMR spectra, DLS and TEM size, and size distribution data. This material is available free of charge via the Internet at <http://pubs.acs.org>.

AUTHOR INFORMATION

Corresponding Author

*E-mail: igivanov@syr.edu (I.G.).

Notes

The authors declare no competing financial interest.

ACKNOWLEDGMENTS

The authors acknowledge the kind assistance of Mr. Robert P. Smith (SUNY ESF) and Prof. Stephan Wilkens (SUNY Upstate Medical University) with the TEM analysis of the dendrimers. Thanks are due to Dr. Hongyi Hu (SUNY ESF) for her help with the theoretical calculations and Prof. Mathew M. Maye (Syracuse University) for the provided access to DLS instrumentation. Partial financial support for this study was granted by NSF (CBET 0853454 and EEC-1156942).

REFERENCES

- (a) *Dendrimers and Other Dendritic Polymers*; Fréchet, J. M. J., Tomalia, D. A., Eds.; John Wiley & Sons, Ltd.: Chichester, UK, 2001.
- (b) Newkome, G. R.; Moorefield, C. N.; Vögtle, F. *Dendrimers and Dendrons: Concepts, Synthesis, Applications*; Wiley-VCH Verlag GmbH: Weinheim, Germany, 2001.
- (c) *Dendrimers: Towards Catalytic, Material and Biomedical Uses*; Caminade, A.-M., Turrin, C.-O., Laurent, R., Ouali, A., Delavaux-Nicot, B., Eds.; John Wiley & Sons, Ltd.: Chichester, UK, 2011.
- (d) Tomalia, D. A.; Christensen, J. B.; Boas, U. *Dendrimers, Dendrons and Dendritic Polymers. Discovery, Applications and the Future*;

- Cambridge University Press: Cambridge, UK, 2012. (e) Mignani, S.; Majoral, J.-P. *New J. Chem.* **2013**, *37*, 3337–3357. (f) Li, Z.; Li, J. *Curr. Org. Chem.* **2013**, *17*, 1334–1349. (g) Wang, D.; Astruc, D. *Coord. Chem. Rev.* **2013**, *257*, 2317–2334 and references therein. (h) Patel, H. N.; Patel, P. M. *Int. J. Pharma Bio Sci.* **2013**, *4*, P454–P463.
- (2) (a) Buhleier, E.; Wehner, W.; Vögtle, F. *Synthesis* **1978**, 155–158. (b) Denkewalter, R. G.; Kolc, J.; Lukasavage, W. J. US Patent 4,289,872, 1979. (c) Newkome, G. R.; Yao, Z. Q.; Baker, G. R.; Gupta, V. K. J. *Org. Chem.* **1985**, *50*, 2003–2004. (d) Tomalia, D. A.; Baker, H.; Dewald, J.; Hall, M.; Kallos, G.; Martin, S.; Roeck, J.; Ryder, J.; Smith, P. *Polym. J.* **1985**, *17*, 117–132.
- (3) (a) Hawker, C. J.; Fréchet, J. M. J. *J. Am. Chem. Soc.* **1990**, *112*, 7638–7647. (b) Miller, T. M.; Neenan, T. X. *Chem. Mater.* **1990**, *2*, 346–349.
- (4) Huisgen, R. *Angew. Chem., Int. Ed. Engl.* **1963**, *2*, 565–598.
- (5) (a) Tornøe, C. W.; Christensen, C.; Meldal, M. J. *Org. Chem.* **2002**, *67* (9), 3057–3064. (b) Rostovtsev, V.; Green, L. G.; Fokin, V. V.; Sharpless, K. B. *Angew. Chem., Int. Ed.* **2002**, *41* (14), 2596–2599.
- (6) (a) Wu, P.; Feldman, A. K.; Nugent, A. K.; Hawker, C. J.; Scheel, A.; Voit, B.; Pyun, J.; Fréchet, J. M. J.; Sharpless, K. B.; Fokin, V. V. *Angew. Chem., Int. Ed.* **2004**, *43*, 3928–3932. (b) Joralemon, M. J.; O'Reilly, R. K.; Matson, J. B.; Nugent, A. K.; Hawker, C. J.; Wooley, K. L. *Macromolecules* **2005**, *38*, 5436–5442. (c) Fernandez-Megia, E.; Correa, J.; Rodriguez-Meizoso, I.; Riguera, R. *Macromolecules* **2006**, *39*, 2113–2120. (d) Ornelas, C.; Aranzaes, J. R.; Salmon, L.; Astruc, D. *Chem.—Eur. J.* **2008**, *14*, 50–64 and references therein.
- (7) (a) Franc, G.; Kakkar, A. *Chem. Commun.* **2008**, 5267–5276. (b) Voit, B. *New J. Chem.* **2007**, *31*, 1139–1151. (c) Walter, M. V.; Malkoch, M. *Chem. Soc. Rev.* **2012**, *41*, 4593–4609.
- (8) (a) Diaz, D. D.; Puna, S.; Holzer, P.; McPherson, A. K.; Sharpless, K. B.; Fokin, V. V.; Finn, M. G. *J. Polym. Sci., Part A: Polym. Chem.* **2004**, *42*, 4392–4403. (b) Takizawa, K.; Nulwala, H.; Thibault, R. J.; Lowenhielm, P.; Yoshinaga, K.; Wooley, K. L.; Hawker, C. J. *J. Polym. Sci., Part A: Polym. Chem.* **2008**, *46*, 2897–2912.
- (9) (a) Parrish, B.; Breitenkamp, R. B.; Emrick, T. *J. Am. Chem. Soc.* **2005**, *127*, 7404–7410. (b) Malkoch, M.; Thibault, R. J.; Drockenmuller, E.; Messerschmidt, M.; Voit, B.; Russell, T. P.; Hawker, C. J. *J. Am. Chem. Soc.* **2005**, *127*, 14942–14949. (c) Liu, X.-M.; Thakur, A.; Wang, D. *Biomacromolecules* **2007**, *8*, 2653–2658. (d) Johnson, J. A.; Finn, M. G.; Koberstein, J. T.; Turro, N. J. *Macromol. Rapid Commun.* **2008**, *29*, 1052–1072. (e) Breed, D. R.; Thibault, R.; Xie, F.; Wang, Q.; Hawker, C. J.; Pine, D. J. *Langmuir* **2009**, *25*, 4370–4376. (f) Pressly, E. D.; Amir, R. J.; Hawker, C. J. *J. Polym. Sci., Part A: Polym. Chem.* **2011**, *49*, 814–819. (g) Lallana, E.; Fernandez-Trillo, F.; Sousa-Hervez, A.; Riguera, R.; Fernandez-Megia, E. *Pharm. Res.* **2012**, *29*, 902–921.
- (10) (a) Badèche, S.; Daran, J. C.; Ruiz, J.; Astruc, D. *Inorg. Chem.* **2008**, *47*, 4903–4908. (b) Crowley, J. D.; Gavey, E. L. *Dalton Trans.* **2010**, *39*, 4035–4037. (c) Kilpin, K. J.; Gavey, E. L.; McAdam, C. J.; Anderson, C. B.; Lind, S. J.; Keep, C. C.; Gordon, K. C.; Crowley, J. D. *Inorg. Chem.* **2011**, *50*, 6334–6346.
- (11) (a) Crowley, J. D.; Bandeen, P. H. *Dalton Trans.* **2010**, *39*, 612–623. (b) Urankar, D.; Pinter, B.; Pevec, A.; De Proft, F.; Turel, I.; Kosmrlj, J. *Inorg. Chem.* **2010**, *49*, 4820–4829. (c) Anderson, C. B.; Elliott, A. B. S.; McAdam, C. J.; Gordon, K. C.; Crowley, J. D. *Organometallics* **2013**, *32*, 788–797.
- (12) Anderson, C. B.; Elliott, A. B. S.; Lewis, J. E. M.; McAdam, C. J.; Gordon, K. C.; Crowley, J. D. *Dalton Trans.* **2012**, *41*, 14625–14632.
- (13) Kilpin, K. J.; Paul, U. S. D.; Lee, A.-L.; Crowley, J. D. *Chem. Commun.* **2011**, *47*, 328–330.
- (14) Crowley, J. D.; Bandeen, P. H.; Hanton, L. R. *Polyhedron* **2010**, *29*, 70–83.
- (15) (a) Maisomial, A.; Serafin, P.; Traikia, M.; Debiton, E.; Théry, V.; Aitken, D. J.; Lemoine, P.; Viossat, B.; Gautier, A. *Eur. J. Inorg. Chem.* **2008**, *2008*, 298–305. (b) Deraedt, C.; Salmon, L.; Ruiz, J.; Astruc, D. *Adv. Synth. Catal.* **2013**, *355*, 2992–3001.
- (16) Mindt, T. L.; Struthers, H.; Brans, L.; Anguelov, T.; Schweinsberg, C.; Maes, V.; Tourré, D.; Schibli, R. *J. Am. Chem. Soc.* **2006**, *128*, 15096–15097.
- (17) Jana, R.; Pathak, T. P.; Sigman, M. S. *Chem. Rev.* **2011**, *111*, 1417–1492.
- (18) (a) Yeung, L. K.; Crooks, R. M. *Nano Lett.* **2001**, *1*, 14–17. (b) Li, Y.; El Sayed, M. A. *J. Phys. Chem. B* **2001**, *105*, 8938. (c) Pittelkow, M.; Moth-Poulsen, K.; Boas, U.; Christensen, J. B. *Langmuir* **2003**, *19*, 7682. (d) Garcia-Martinez, J. C.; Lezutekong, R.; Crooks, R. M. *J. Am. Chem. Soc.* **2005**, *127*, 5097–5103. (e) Snelders, D. J. M.; van Koten, G.; Gebbink, R. J. M. *J. Am. Chem. Soc.* **2009**, *131*, 11407–11416. (f) Bagul, R. S.; Jayaraman, N. *J. Organomet. Chem.* **2012**, *701*, 27–35. (g) Xu, Y.; Zhang, Z.; Zheng, J.; Du, Q.; Li, Y. *Appl. Organomet. Chem.* **2013**, *27*, 13–18. for general reviews on metalloendrimers see: El Kazzaoui, S.; El Brahmi, N.; Mignani, S.; Bousmina, M.; Zablocka, M.; Majoral, J.-P. *Curr. Med. Chem.* **2012**, *19*, 4995–5010. Tang, Y.-H.; Huang, A.Y.-T.; Chen, P. Y.; Chen, H.-T.; Kao, C.-L. *Curr. Pharm. Des.* **2011**, *17*, 2308–2330. Hwang, S.-H.; Shreiner, C. D.; Moorefield, C. N.; Newkome, G. R. *New J. Chem.* **2007**, *31*, 1192–1217. van Manen, H. J.; van Veggel, F. C. J. M.; Reinhoudt, D. N. Non-covalent synthesis of metalloendrimers. *Top. Curr. Chem.* **2001**, *217*, 121–162.
- (19) For an important review of groundbreaking studies on triazole-containing dendrimers and their metal-binding properties and applications, see: Astruc, D.; Liang, L.; Rapakousiou, A.; Ruiz, J. *Acc. Chem. Res.* **2012**, *45*, 630–640 and references therein.
- (20) It should be noted that thiazolyl dendrimers have also been successfully employed as efficient and recyclable catalysts of Suzuki-Miyaura coupling reactions: Keller, M.; Hameau; Spataro, G.; Ladeira, S.; Caminade, A.-M.; Majoral, J.-P.; Ouali, A. *Green Chem.* **2012**, *14*, 2807–2815 and references therein.
- (21) (a) Fujihara, T.; Yoshida, S.; Ohta, H.; Tsuji, Y. *Angew. Chem., Int. Ed.* **2008**, *47*, 8310–8313. (b) Gähler, C.; Jeschke, J.; Nurgazina, G.; Dietrich, S.; Schaarschmidt, D.; Georgi, C.; Schlesinger, M.; Mehring, M.; Lang, H. *Catal. Lett.* **2013**, *143*, 317–323. (c) Deraedt, C.; Salmon, L.; Etienne, L.; Ruiz, J.; Astruc, D. *Chem. Commun.* **2013**, *49*, 8169–8171.
- (22) Moore, J. S.; Stupp, S. I. *Macromolecules* **1990**, *23*, 65–70.
- (23) *Density Functional Methods in Chemistry*; Labanowski, J. K., Andzelm, J., Eds.; Springer Verlag: New York, 1991.
- (24) Becke, A. D. *J. Chem. Phys.* **1993**, *98*, 5648–5652.
- (25) (a) Hay, P. J.; Wadt, W. R. *J. Chem. Phys.* **1985**, *82*, 299–310. (b) Bakalova, A.; Varbanov, H.; Stanchev, S.; Ivanov, D.; Jensen, F. *Int. J. Quantum Chem.* **2009**, *109*, 826–836 and references therein.
- (26) Hehre, W. J.; Radom, L.; von R. Schleyer, P.; Pople, J. A. *Ab Initio Molecular Orbital Theory*; Wiley: New York, 1986.
- (27) Gaussian 09, Revision A.02: Frisch, M. J.; Trucks, G. W.; Schlegel, H. B.; Scuseria, G. E.; Robb, M. A.; Cheeseman, J. R.; Scalmani, G.; Barone, V.; Mennucci, B.; Petersson, G. A.; Nakatsuji, H.; Caricato, M.; Li, X.; Hratchian, H. P.; Izmaylov, A. F.; Bloino, J.; Zheng, G.; Sonnenberg, J. L.; Hada, M.; Ehara, M.; Toyota, K.; Fukuda, R.; Hasegawa, J.; Ishida, M.; Nakajima, T.; Honda, Y.; Kitao, O.; Nakai, H.; Vreven, T.; Montgomery, J. A., Jr.; Peralta, J. E.; Ogliaro, F.; Bearpark, M.; Heyd, J. J.; Brothers, E.; Kudin, K. N.; Staroverov, V. N.; Kobayashi, R.; Normand, J.; Raghavachari, K.; Rendell, A.; Burant, J. C.; Iyengar, S. S.; Tomasi, J.; Cossi, M.; Rega, N.; Millam, J. M.; Klene, M.; Knox, J. E.; Cross, J. B.; Bakken, V.; Adamo, C.; Jaramillo, J.; Gomperts, R.; Stratmann, R. E.; Yazayev, O.; Austin, A. J.; Cammi, R.; Pomelli, C.; Ochterski, J. W.; Martin, R. L.; Morokuma, K.; Zakrzewski, V. G.; Voth, G. A.; Salvador, P.; Dannenberg, J. J.; Dapprich, S.; Daniels, A. D.; Farkas, O.; Foresman, J. B.; Ortiz, J. V.; Cioslowski, J.; Fox, D. J. Gaussian, Inc.: Wallingford, CT, 2009.
- (28) (a) Dingels, C.; Schömer, M.; Frey, H. *Chem. Unserer Zeit* **2011**, *45*, 338–349. (b) Harris, J. M.; Zalipsky, S., Eds.; *Poly(ethylene glycol): Chemistry and Biological Applications*; ACS Symp. Ser., Vol. 680; American Chemical Society: Washington, DC, 1997. (c) Bailey, F. E., Jr.; Koleske, J. V., Eds.; *Alkylene Oxides and Their Polymers*; Marcel Dekker, Inc.: New York, 1991.
- (29) (a) Liu, M.; Kono, K.; Fréchet, J. M. J. *J. Polym. Sci., Part A: Polym. Chem.* **1999**, *37*, 3492–3503. (b) Gillies, E. R.; Fréchet, J. M. J. *J. Am. Chem. Soc.* **2002**, *124*, 14137–14146. (c) Gillies, E. R.; Dy, E.; Fréchet, J. M. J.; Szoka, F. C. *Mol. Pharmaceutics* **2005**, *2*, 129–138. (d) Morara, A. D.; McCarley, R. L. *Org. Lett.* **2006**, *8*, 1999–2002. (e) Gajbhiye, V.;

Kumar, P. V.; Tekade, R. K.; Jain, N. K. *Curr. Pharm. Des.* **2007**, *13*, 415–429. (f) Kaminskas, L. M.; Boyd, B. J.; Karella, P.; Krippner, G. Y.; Lessene, R.; Kelly, B.; Porter, C. J. H. *Mol. Pharmaceutics* **2008**, *5*, 449–463. (g) Lim, J.; Guo, Y.; Rostollan, C. L.; Stanfield, J.; Hsieh, J.-T.; Sun, X.; Simanek, E. E. *Mol. Pharmaceutics* **2008**, *5*, 540–547. (h) Cheng, Y.; Zhao, L.; Li, Y.; Xu, T. *Chem. Soc. Rev.* **2011**, *40*, 2673–2703 and references therein.

(30) (a) Newkome, G. R.; Kotta, K. K.; Mishra, A.; Moorefield, C. N. *Macromolecules* **2004**, *37*, 8262–8268. (b) Feng, X.; Taton, D.; Borsali, R.; Chaikof, E. L.; Gnanou, Y. *J. Am. Chem. Soc.* **2006**, *128*, 11551–11562. (c) Feng, X.; Taton, D.; Chaikof, E. L.; Gnanou, Y. *Macromolecules* **2009**, *42*, 7292–7298. (d) Dhanikula, R. S.; Hildgen, P. *Bioconjugate Chem.* **2005**, *17*, 29–41. (e) Dhanikula, R. S.; Hildgen, P. *Biomaterials* **2007**, *28*, 3140–3152. (f) Arseneault, M.; Levesque, I.; Morin, J. F. *Macromolecules* **2012**, *45*, 3687–3694.

(31) (a) Ihre, H.; Hult, A.; Söderlind, E. *J. Am. Chem. Soc.* **1996**, *118*, 6388–6395. (b) Ihre, H.; Hult, A.; Fréchet, J. M. J.; Gitsov, I. *Macromolecules* **1998**, *31*, 4061–4068. (c) Ihre, H.; Padilla de Jesus, O. L.; Fréchet, J. M. J. *J. Am. Chem. Soc.* **2001**, *123*, 5908–5917. (d) Malkoch, M.; Malmström, E.; Hult, A. *Macromolecules* **2002**, *35*, 8307–8314. (e) Calmark, A.; Malmström, E.; Malkoch, M. *Chem. Soc. Rev.* **2013**, *42*, 5858–5879 and references therein.

(32) (a) Padilla de Jesus, O. L.; Ihre, H. R.; Gagne, L.; Fréchet, J. M. J.; Szoka, F. C. *Bioconjugate Chem.* **2002**, *13*, 453–461. (b) Wu, Z.; Zheng, X.; Zhang, Y.; Felin, N.; Lundberg, P.; Fadeel, B.; Malkoch, M.; Nyström, A. M. *J. Polym. Sci., Part A: Polym. Chem.* **2012**, *50*, 217–226. (c) Hed, Y.; Zhang, Y.; Andrén, O. C. J.; Zeng, X.; Nyström, A. M.; Malkoch, M. *J. Polym. Sci., Part A: Polym. Chem.* **2013**, *51*, 3993–3996.

(33) Other PEG containing polymers have shown similar low molecular mass tailing on the same SEC column set and identical analysis conditions: Gitsov, I.; Johnson, F. E. *J. Polym. Sci., Part A: Polym. Chem.* **2008**, *46*, 4130–4139.

(34) Ma, X. P.; Zhou, Z. X.; Jin, E. L.; Sun, Q. H.; Zhang, B.; Tang, J. B.; Shen, Y. Q. *Macromolecules* **2013**, *46*, 37–42.

(35) (a) Metin, Ö.; Durap, F.; Aydemir, M.; Özkar, S. *J. Mol. Catal. A: Chem.* **2011**, *337*, 39–44. (b) Ogasawara, S.; Kato, S. *J. Am. Chem. Soc.* **2010**, *132*, 4608–4613.

(36) (a) Štěpnička, P.; Schneiderová, B.; Schulz, J.; Cisařová, I. *Organometallics* **2013**, *32*, 5754–5765. (b) Fihri, A.; Luart, D.; Leu, C.; Solhy, A.; Chevrin, C.; Polshettiwar, V. *Dalton Trans.* **2011**, *40*, 3116–3121. (c) Fihri, A.; Bouhrara, M.; Nekoueishahraki, B.; Basset, J.-M.; Polshettiwar, V. *Chem. Soc. Rev.* **2011**, *40*, 5181–5203 and references therein.

(37) (a) Wu, W.-Y.; Chen, S.-N.; Tsai, F. Y. *Tetrahedron Lett.* **2006**, *47*, 9267–9270. (b) Mejías, N.; Pleixats, R.; Shafir, A.; Medio-Simón, M.; Asensio, G. *Eur. J. Org. Chem.* **2010**, 5090–5099.

(38) (a) Len, C.; Hedhili, M. N.; Fihri, A. *Appl. Catal., A* **2013**, *450*, 13–18. (b) Wang, L.; Cai, C. *J. Mol. Catal. A: Chem.* **2009**, *306*, 97–101.

(39) Jamwal, N.; Gupta, M.; Paul, S. *Green Chem.* **2008**, *10*, 999–1003.

(40) Godoy, F.; Segarra, C.; Poyatos, M.; Peris, E. *Organometallics* **2011**, *30*, 684–688.

(41) Zhou, C.; Wang, J.; Li, L.; Wang, R.; Hong, M. *Green Chem.* **2011**, *13*, 2100–2106.